General Disclaimer

One or more of the Following Statements may affect this Document

- This document has been reproduced from the best copy furnished by the organizational source. It is being released in the interest of making available as much information as possible.

- This document may contain data, which exceeds the sheet parameters. It was furnished in this condition by the organizational source and is the best copy available.

- This document may contain tone-on-tone or color graphs, charts and/or pictures, which have been reproduced in black and white.

- This document is paginated as submitted by the original source.

- Portions of this document are not fully legible due to the historical nature of some of the material. However, it is the best reproduction available from the original submission.

JPL PUBLICATION 77-65

Development of a Multiplexed Bypass Control System for Aerospace Batteries

National Aeronautics and
Space Administration

Jet Propulsion Laboratory
California Institute of Technology
Pasadena, California 91103

JPL PUBLICATION 77-65

Development of a Multiplexed Bypass Control System for Aerospace Batteries

H. A. Frank

November 1, 1977

National Aeronautics and
Space Administration

Jet Propulsion Laboratory
California Institute of Technology
Pasadena, California 91103

PREFACE

The work described in this report was performed by the Control and Energy Conversion Divison of the Jet Propulsion Laboratory.

ACKNOWLEDGEMENT

The bypass system described herein was designed by former JPL contract employee Mr. John Bennett. Significant contributions were also made by Mr. A.P. Wagner and Mr. Jack Lepisto, part-time student employee.

ABSTRACT

A breadboard bypass control system was developed to control a battery comprised of 26 JPL-developed Negative Limited Ni-Cd cells. The system was designed to automatically remove cells from the circuit when their voltages exceeded a fixed limit on charge and fell below a fixed limit on discharge. Major components of the system consisted of a cell voltage monitor, a multiplexing circuit, and individual electromechanical relays for each cell. The system was found to function well in controlling the battery during a simulated 10-month MM-71 mission and a 2-month simulated low earth orbit cycling mission. A flight version of the bypass system is estimated to have a total parts count of 150 and total weight of 1.63 kg. When fully developed, the system shows promise for improving life and reliability of spacecraft batteries. The technology developed on this project is recommended for transfer to the on-going Automated Power Systems Management Program.

CONTENTS

FIGURES

FIGURES (contd)

SECTION I

INTRODUCTION

Designers and users of aerospace batteries are quite concerned about the problem area of cell imbalance, i.e., when the capacities of one or more cells differ from the capacity of other cells in a battery. Reasons for this concern are twofold. First, the cell or cells with lowest capacity become fully charged before the others during a charge period and begin to evolve gases internally. Second, the cell or cells with lowest capacity become fully discharged before the others during a discharge period and reach the condition of overdischarge or reversal, wherein they also begin to evolve gases internally. In either case the cells with lowest capacity exhibit internal gassing. The amount of gassing varies, depending on magnitude and time duration of the charge or discharge current, and the degree of imbalance between the cells. At very low rates of charge and discharge and for short time periods as well as with a small degree of cell imbalance, the amount of gassing is quite small and the battery should continue to function normally. At very high rates of charge and discharge and for extended periods of time with a high degree of cell imbalance, the amount of gassing is quite large and results in appreciable rise in internal pressure of the low capacity cell or cells. In some cases, the amount of gassing may be so extensive as to cause rupture of the sealed cell or cells and subsequent catastrophic battery failure.

For the above reasons, the designers and users of sealed aerospace batteries take every precaution to insure that the cells of a particular

battery are as closely matched in capacity as possible. Achievement of this condition requires adherence to rigid quality control procedures during manufacturing, adherence to uniform handling and test procedures for all cells and, finally, thorough screening of the cells before assembly into a battery.

These precautionary measures are usually adequate to insure that the battery cells remain in balance and do not gas internally during the early part their design life.

However, during the later stages of life, these conditions do not always prevail, and the condition of imbalance can and usually does occur. This is attributed to the fact that all cells degrade with time and use, but not necessarily at the same rate. Consequently, during the later stages of life there is a trend toward development of imbalance and the threat of catastrophic battery failure.

One method of avoiding this potential failure mode is to employ a device known as individual cell bypass control. This device functions on a characteristic of low capacity cells which is that they always exhibit a change in voltage immediately preceding the condition of overcharge or overdischarge. In the former case, the cell voltage rises; in the latter case, the cell voltage declines. These changes in voltage (in either direction) can be used to trigger a bypass relay that automatically removes the cell from the battery circuit and therby avoids overcharge or overdischarge.* The development and test of such a bypass control system is the subject of this investigation.

---

*In order to maintain bus voltage within prescribed limits on discharge, the circuit would be modified to replace failed calls with spare charged cells. This modification was not within the scope of this investigation.

SECTION II

DESIGN SPECIFICATIONS

It was necessary to generate a set of design specifications for the battery sub-system to define the requirements for the battery bypass control. A listing of these specifications is given below.

A. TYPE OF BATTERY

The battery type to be used with the battery bypass control was specified as the JPL-developed Negative Limited Ni-Cd Battery(1). This battery differs from conventional Ni-Cd batteries in that its cells contain more positive than negative active materials, and its negative grids are made of silver rather than nickel. These features cause the individual cell voltages to exhibit a sharp and distinct voltage rise at the point of 100% charge input. The voltage rise is much sharper than for conventional Ni-Cd cells at this point, i.e., several hundred millivolts vs about 50 millivolts. The cells were designed by a vendor to have capacities of 20 A-h. Laboratory tests at JPL revealed that their capacities were appreciably degraded (from 20 A-H to 6-15 A-h).

B. CHARGE AND DISCHARGE CURRENTS

It was specified that the system be capable of handling currents up to the "C" rate, or 20 amp, for both charge and discharge.

C. UPPER AND LOWER CUTOFF VOLTAGES

It was specified that a cell be taken out of the charge circuit when its voltage exceeded 1.75 $\pm$ .05 volts (prior tests had established that at this voltage this type of cell was fully charged and was approaching the point of hydrogen evolution). It was specified that a cell be taken out of the discharge circuit when its voltage dropped to 0.90 $\pm$ .05 volts. (Prior tests had established that at this voltage the cell was almost completely discharged and was rapidly approaching the point of reversal.)

D. REINSERTION OF CELLS

It was specified that once a cell had been removed from the circuit on charge, it should remain out of the circuit until the subsequent discharge period. At this point, the cell was to be automatically reinserted into the circuit for the discharge period. Similarly, once a cell had been removed from the circuit on discharge, it was to remain out of the circuit until the beginning of the next charge period. At this point, the cell was to be automatically reinserted in the circuit for the charge period.

E. OPERATING TEMPERATURE

Ambient temperature operating range was specified as 4°C to 32°C (40°F to 90°F.)

F. SIZE, WEIGHT, AND PARTS COUNT

No limit was set on size, weight, and parts count of the system. It was specified, however, that these characteristics be kept to a minimum.

G. NUMBER OF CELLS IN BATTERY

It was specified that initial developmental efforts were to be carried out on a 5-cell battery pack. The final system, however, was to be designed to control a 26-cell battery pack.

SECTION III

INITIAL DESIGN CONCEPTS

The first question to be resolved was whether to employ electromechanical relays or solid state switches to remove the cells from the circuit. Initial preference was given to the solid state switches due to their potentially lower weight and higher reliability characteristics. Subsequent study, however, revealed that the power consumption of solid state switches would be quite high in this application, and this would tend to detract significantly from their claimed advantages. On this basis, it was decided to employ electromechanical relays.

At this point, three control schemes were devised, employing the electromechanical switches and cell voltage monitors. The latter are window comparators which insure cell bypassing when cell voltage is outside a predetermined voltage limit (in this case, 0.9 $\pm$ .05 to 1.75 $\pm$ .05 volts). The control schemes are shown in Figs. 3-1, 3-2, and 3-3 and are described below.

Scheme "A" (Fig. 3-1) employs an individual cell voltage monitor with a floating AC supply for each cell. Advantages of this scheme are: a) no large common mode voltage is present, b) does not need tightly matched resistors, and c) consumes approximately 50% less power than Scheme "B" (below) with DC supply. Disadvantages of Scheme "A" are: a) requires an external AC supply, and b) uses magnetic circuit elements.

Scheme "B" (Fig. 3-2) employs an individual cell voltage monitor, with a DC supply for each cell. Advantages of this scheme are: a) does not require an AC supply, and b) has no magnetic circuit

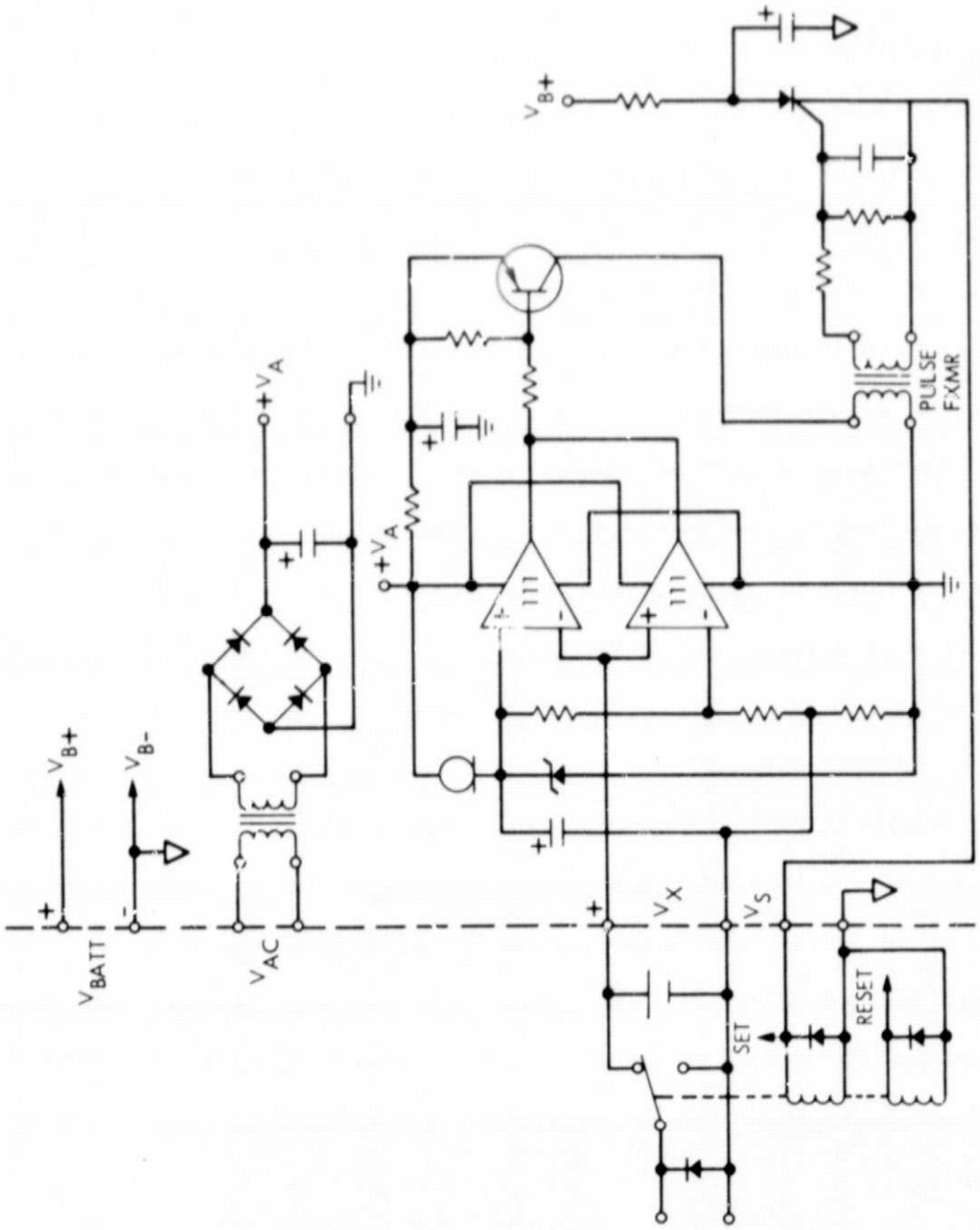

Figure 3-1. Scheme "A", Individual Cell Voltage Monitor (Floating Supply)

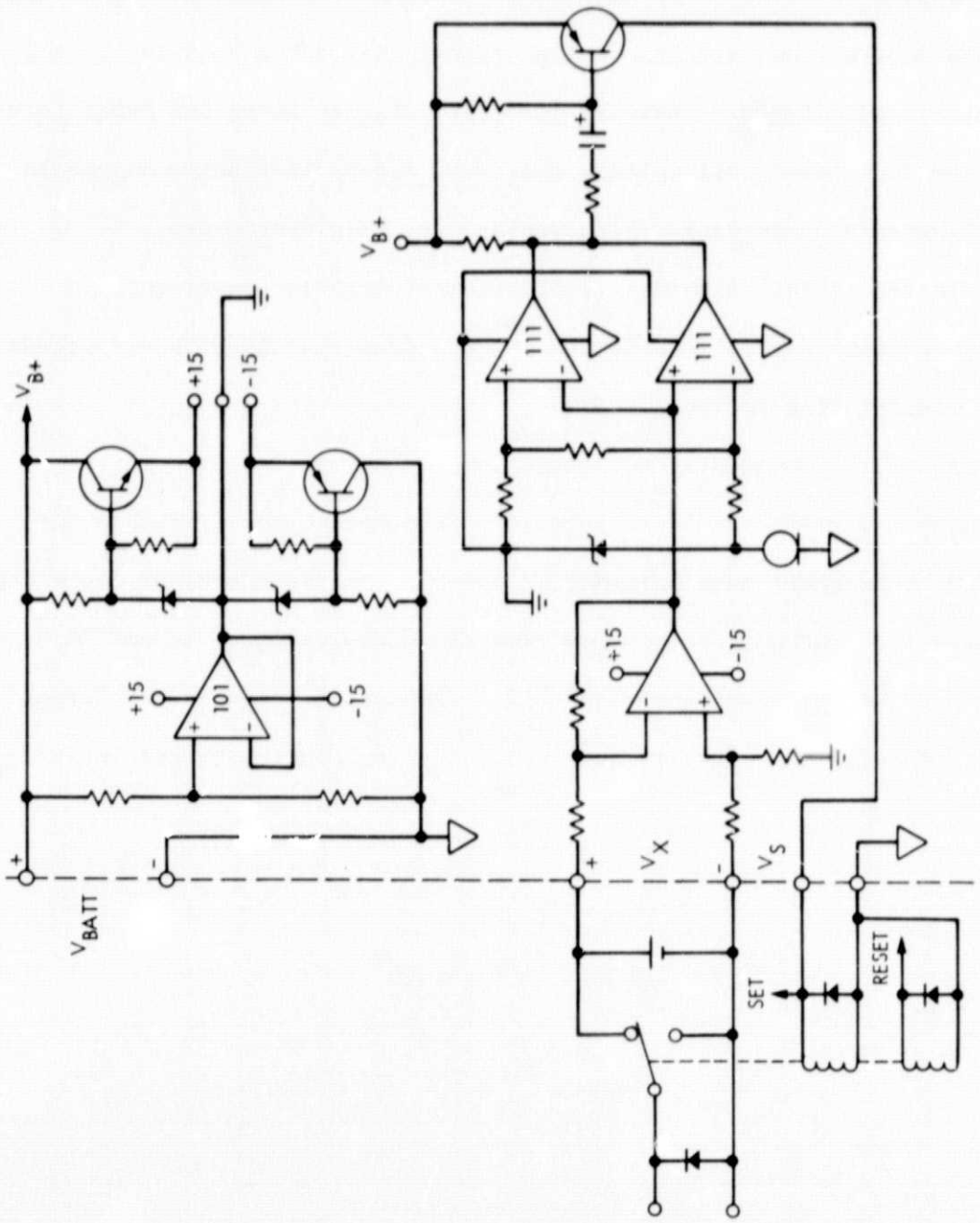

Figure 3-2. Scheme "B", Individual Cell Voltage Monitor (DC Supply)

elements. Disadvantages of this scheme are: a) requires four tightly matched ultra-high stability resistors, and b) requires approximately twice the power consumption of Scheme "A" with floating AC supply.

Scheme "C" (Fig. 3-3) employs a floating AC supply, a single cell voltage monitor, and a multiplexing circuit that scans individual cell voltages. Advantages of this scheme are: a) uses about 50% fewer parts than the individual cell voltage monitors, and b) is readily adaptable to telemetering interface. Disadvantages of this scheme are: a) increased circuit complexity, b) requires negative power supply, and c) requires specialized design to interface readily with any preset power conditioning design concept.

As will subsequently be shown, Scheme "A" was selected for a preliminary 5-cell breadboard because it was deemed more reliable and required less power than Scheme "B," and the limited number of cells did not appear to warrant the complexities of multiplexing of Scheme "C." Scheme "C" was selected for a 26-cell breadboard in view of the larger number of cells and significantly reduced parts count with multiplexing.

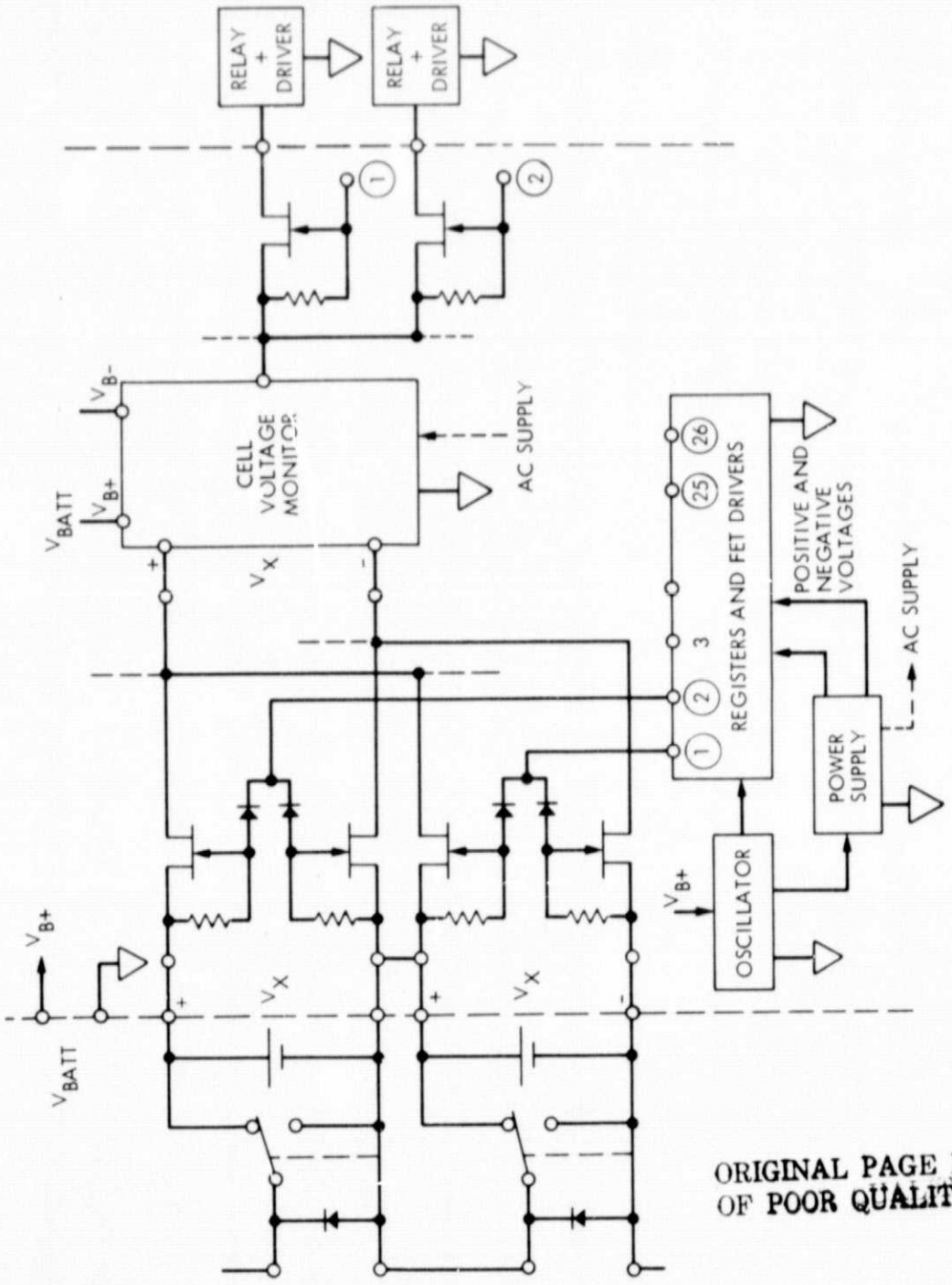

Figure 3-3. Scheme "C", Cell Voltage Monitor (Multiplexing)

ORIGINAL PAGE IS
OF POOR QUALITY

SECTION IV

5-CELL BATTERY BREADBOARD

As a preliminary step, it was decided to develop and test a bypass system for a 5-cell battery pack of Negative Limited Ni-Cd cells. Control Scheme "A" (with individual cell voltage monitors for each cell and a floating AC supply) was selected for this purpose. Figure 4-1 provides details of the electronic design of this 5-module assembly. Parts count was 35 parts/cell, and weight was 104 g/cell, including relays. Each module was identical and designed to bypass charge current when cell voltage exceeded 1.75 $\pm$ .05 volts and to bypass discharge current when cell voltage decreased below 0.90 $\pm$ .05 volts. The modules were designed to operate on 50 VAC at 2.4 KHz, such as employed on prior spacecraft. Power consumption per module was 50 milliwatts in the "normal" or so called "standby" condition and 155 milliwatts in the so called "bypass" or "cutoff" condition. The circuit provides for permanent hold until reset of any cell that has reached the bypass condition in either direction. Reset can be carried out either manually or remotely and automatically with a signal from a clock or timer. A photograph of one of the assembled cell voltage monitors is given in Figure 4-2. Components are assembled on a card approximately 11.4 cm long and 7.0 cm wide. A photograph of the completed breadboard, including the Negative Limited cells, is given in Figure 4-3. In addition to a cell voltage monitor, each cell was equipped with a pressure transducer. These transducers were used for measurement purposes only and were not connected to the control system.

The 5-cell breadboard assembly was first subjected to preliminary electrical tests to check functionality of the components. All components were found to function as designed, so the assembly was then placed on a variety of cycle regimes to test functionality of the bypass system. The regimes included intentional periods of overcharge and overdischarge to drive cell voltages out of prescribed limits and observe response of the bypass system. Results shown in Figure 4-4 revealed that the system operated well and as planned by removing a cell from the circuit when it reached 1.75 volts on charge and 0.90 volts on discharge.

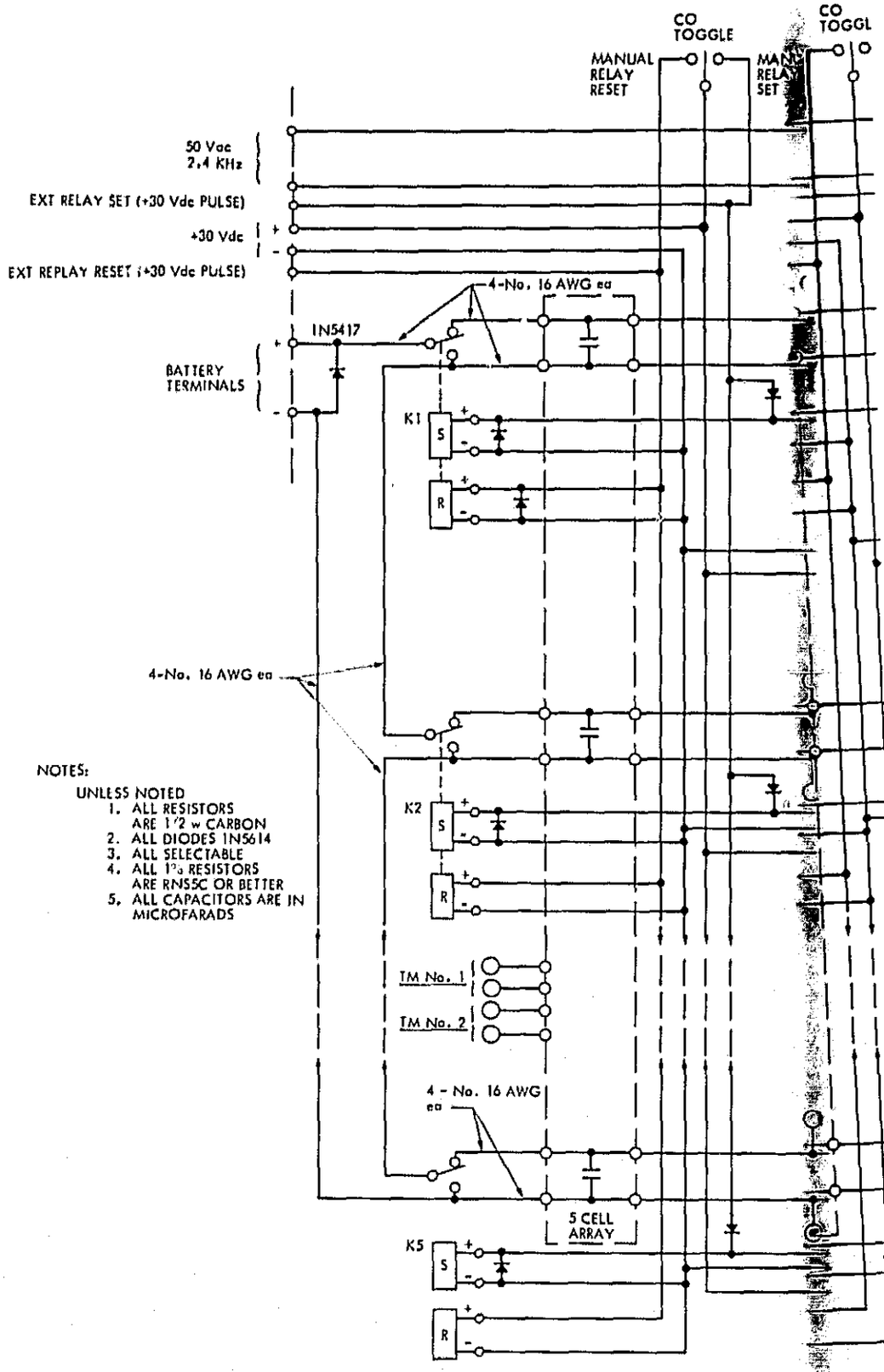

NOTES:

UNLESS NOTED

1. ALL RESISTORS ARE 1/2 w CARBON
2. ALL DIODES 1N5614
3. ALL SELECTABLE
4. ALL 1% RESISTORS ARE RNS5C OR BETTER
5. ALL CAPACITORS ARE IN MICROFARADS

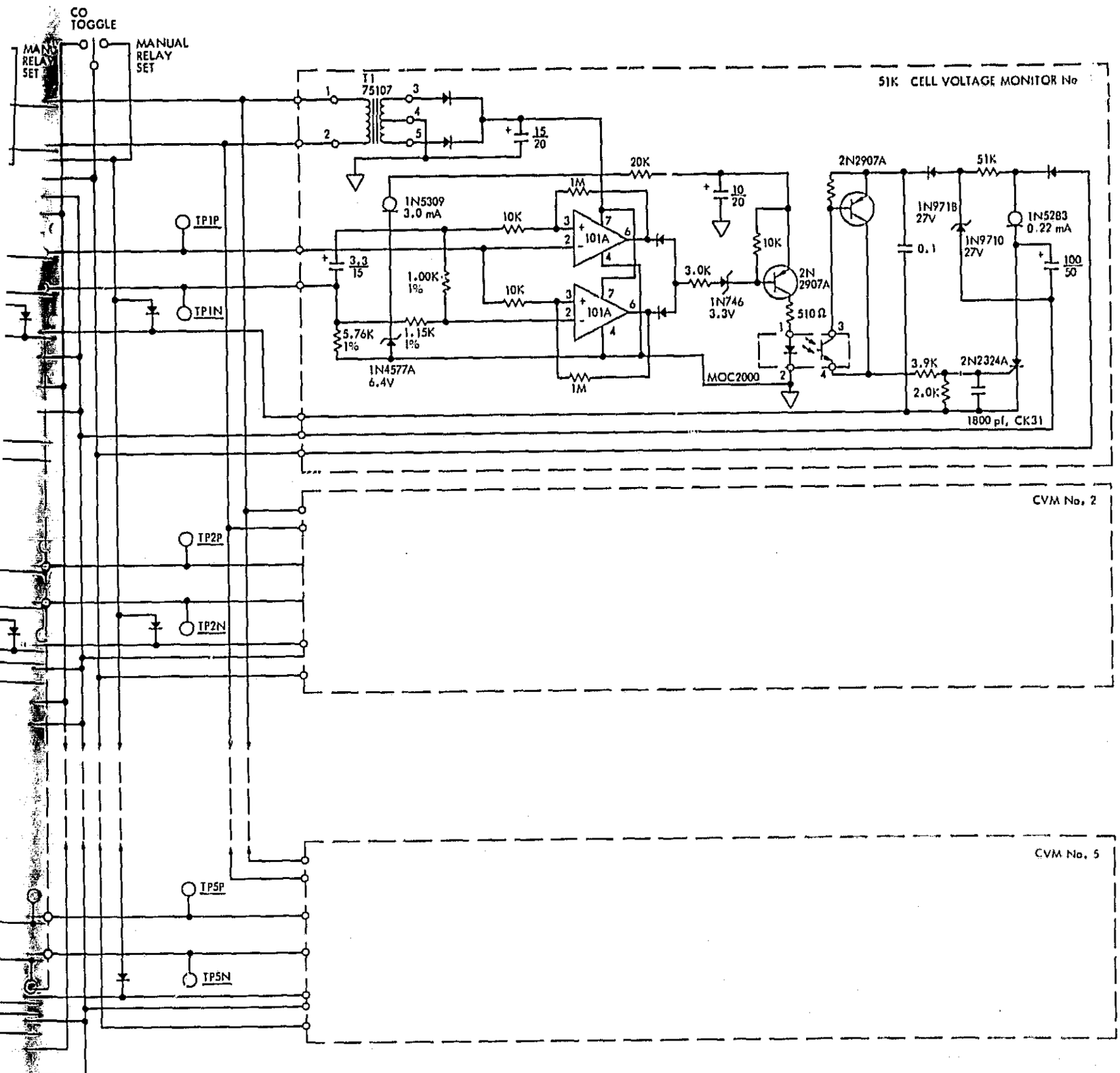

Figure 4-1. Bypass Control Circuit for 5-Cell Battery Pack

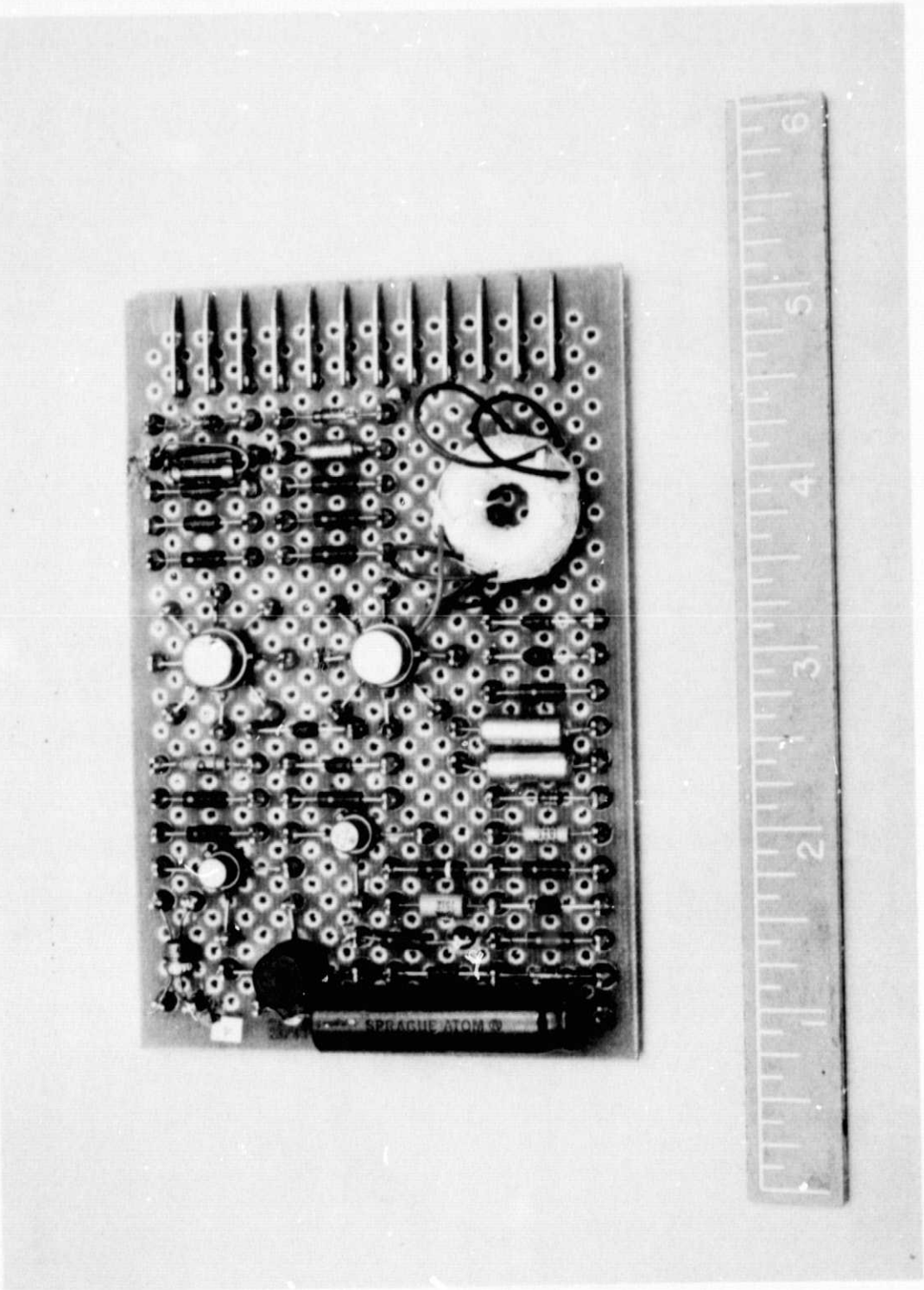

Figure 4-2. Cell Voltage Monitor

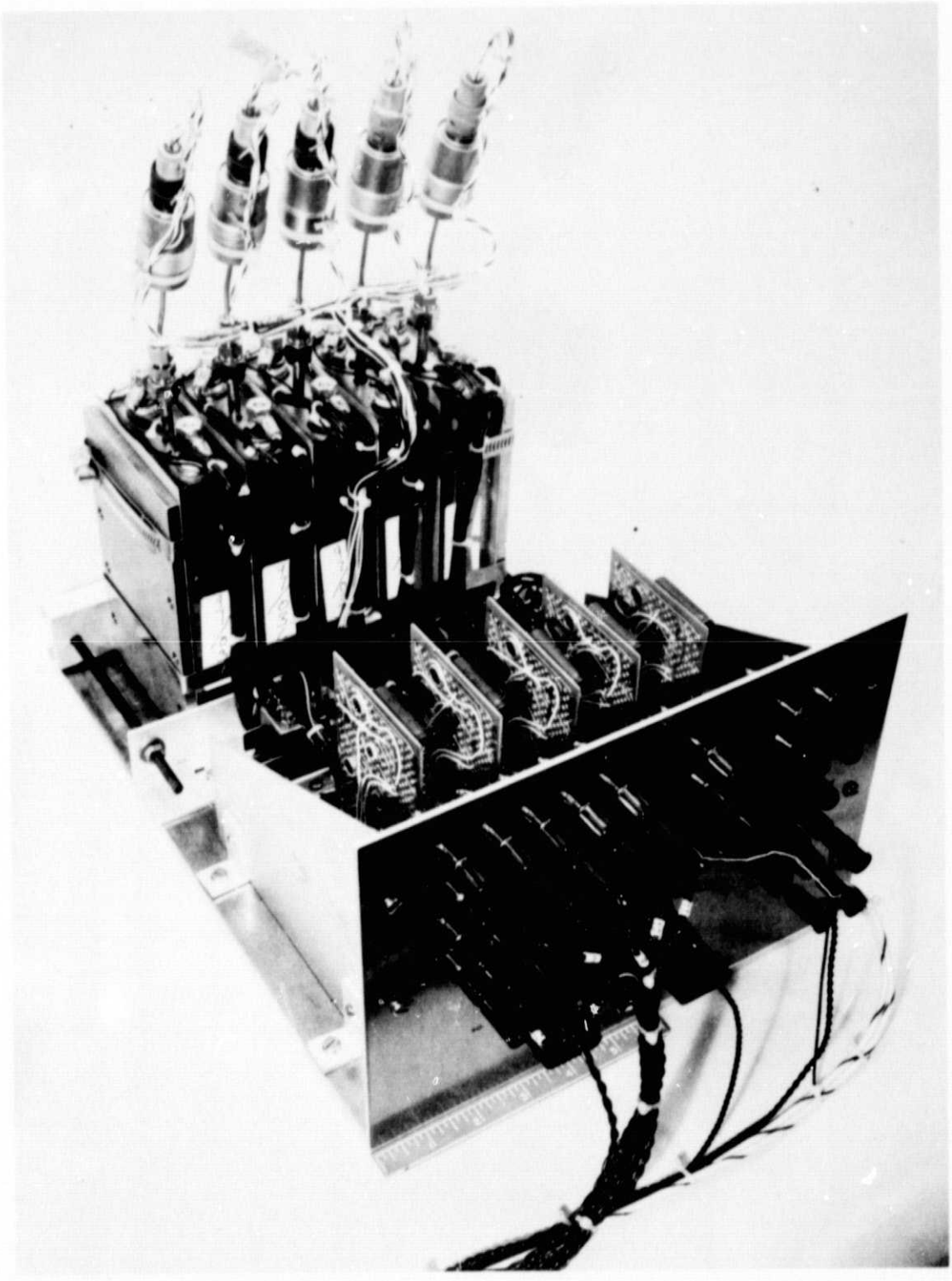

Figure 4-3. Breadboard of 5-Cell Negative Limited Ni-Cd Battery

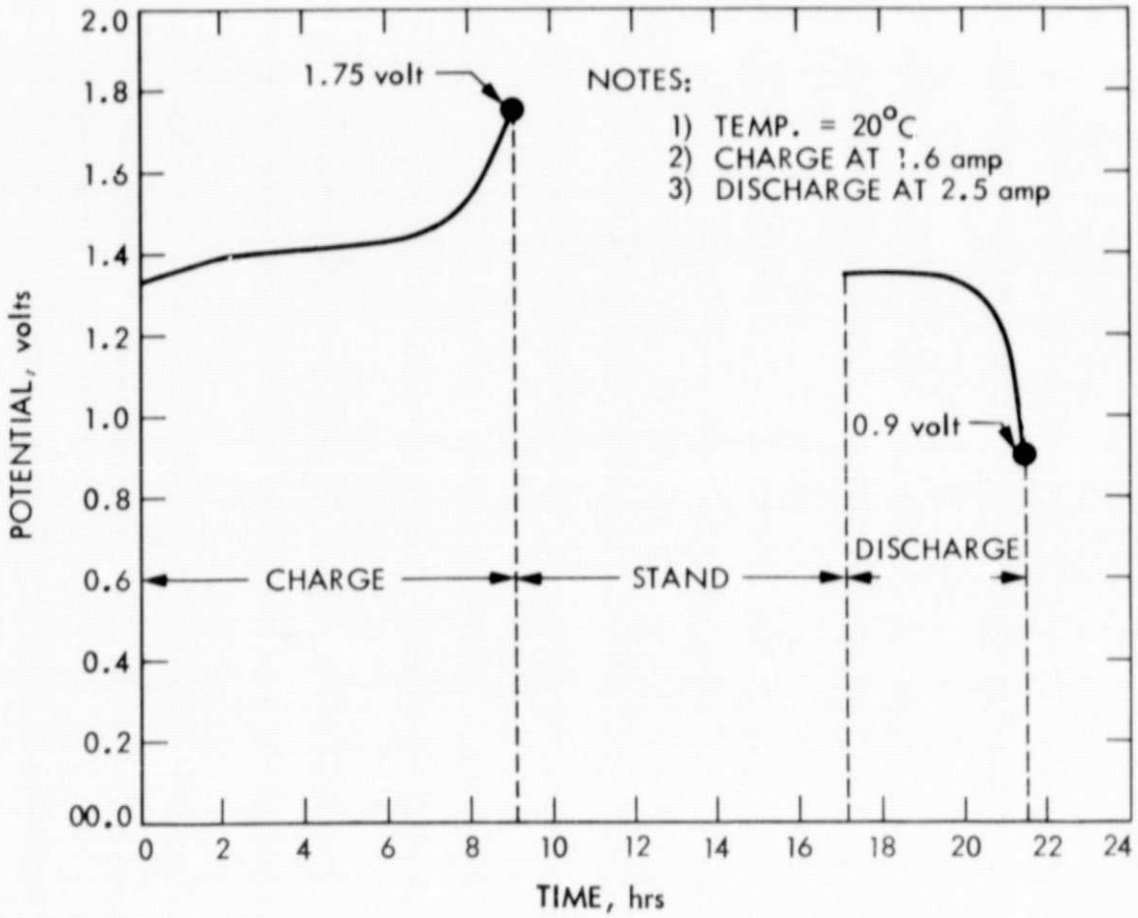

Figure 4-4. Voltage Trace of One Cell in 5-Cell Pack during Course of Complete Charge-Discharge Cycle

ORIGINAL PAGE IS
OF POOR QUALITY

SECTION V

26-CELL BATTERY BREADBOARD

The next step involved development and test of a bypass system for a full-scale (26-cell) battery similar to those employed on prior spacecraft. The system was to be designed in breadboard fashion to control 26 Negative Limited Ni-Cd cells as above.

A. DEVELOPMENT

Control Scheme "C" (multiplexed cell voltage monitor with floating AC supply) was deemed most appropriate for the 26-cell breadboard on the basis that this scheme would require significantly fewer parts than either Schemes "A" or "B." On this basis, a control system was designed in accordance with Scheme "C."

The general operating principles of the system were to be as follows. First, a multiplexer sequentially applies each cell voltage to a single cell voltage monitor. Next, the cell voltage monitor measures the voltage of each cell. Finally, the cell voltage monitor triggers a cell bypass relay if a cell's voltage is outside preset limits.

The system that was designed to perform these functions is given in Figures 5-1 through 5-9 and is described below. Figure 5-1 is a block diagram of the complete system. Figure 5-2 is a diagram of the multiplexer timing. Figure 5-3 is a schematic diagram of the multiplexer. Figure 5-4 is a circuit diagram of the cell voltage monitor. Figure 5-4 is a schematic diagram of the Field Effect Transistor (FET) switch and driver board. Figure 5-6 is a schematic diagram of the 2-channel FET switch and driver board. Figure 5-7 is a detailed

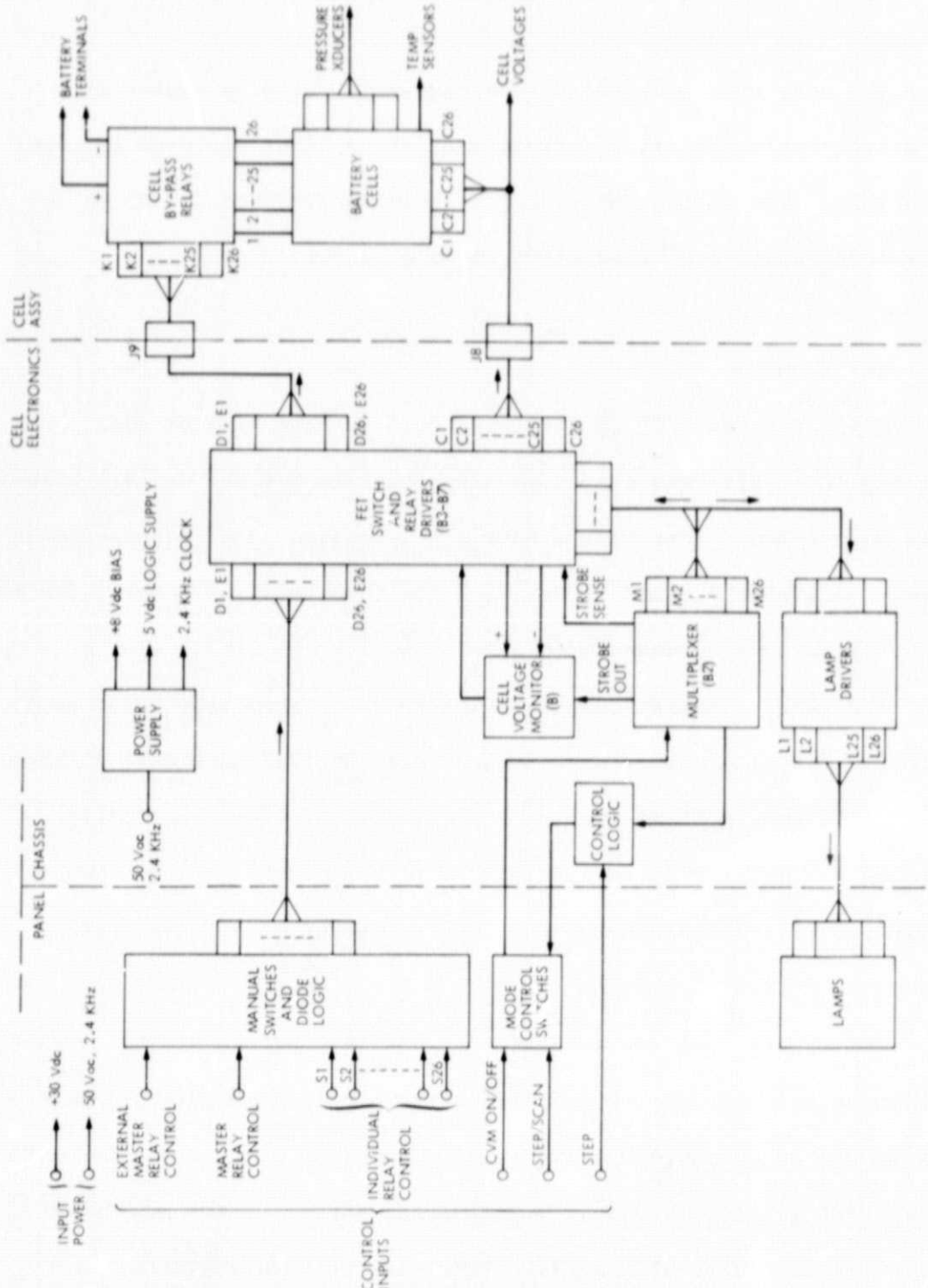

Figure 5-1. Block Diagram - Breadboard Negative Limited Battery Charge Control System

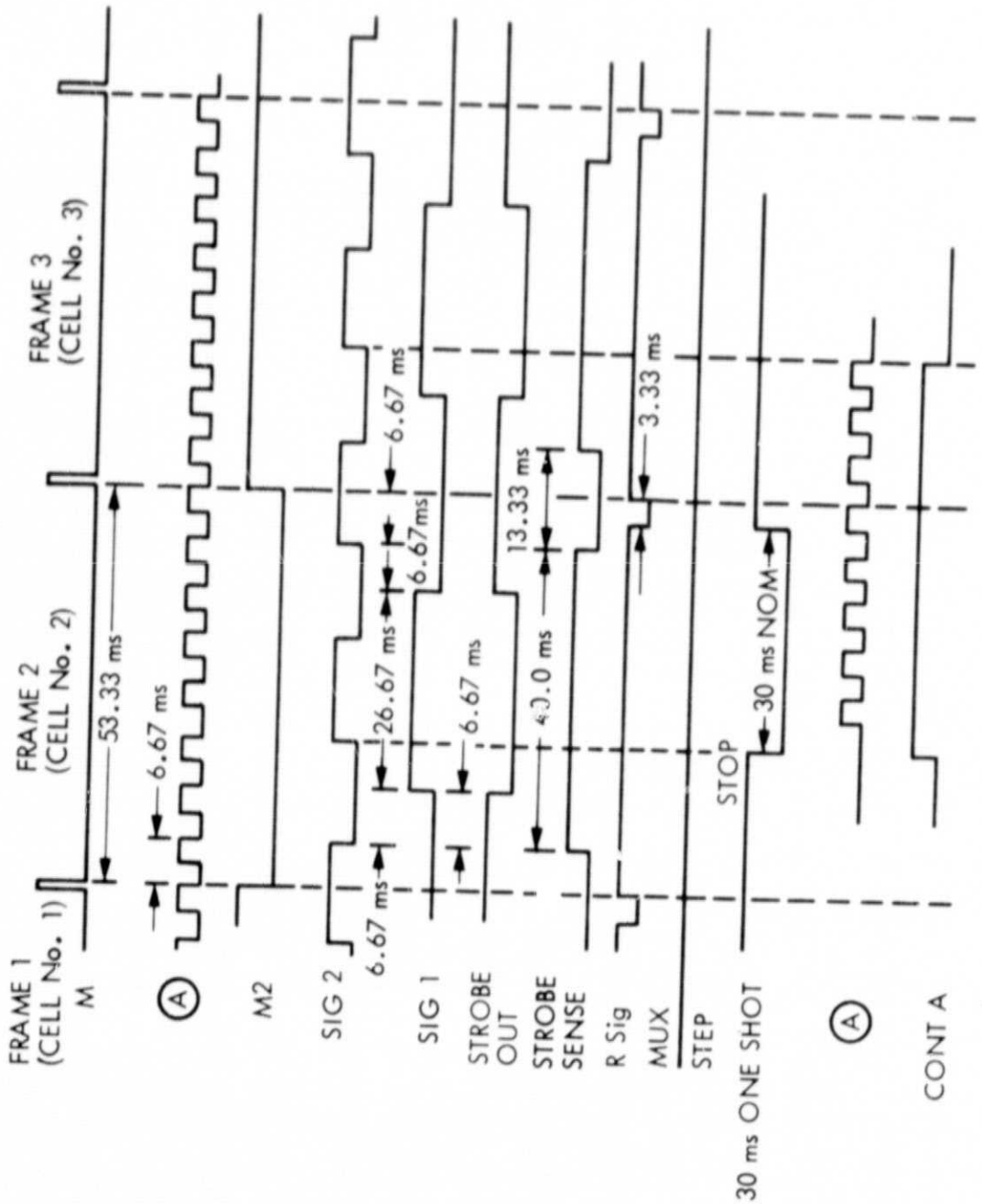

Figure 5-2. Multiplexer Logic

FOLDOUT FRAME 1

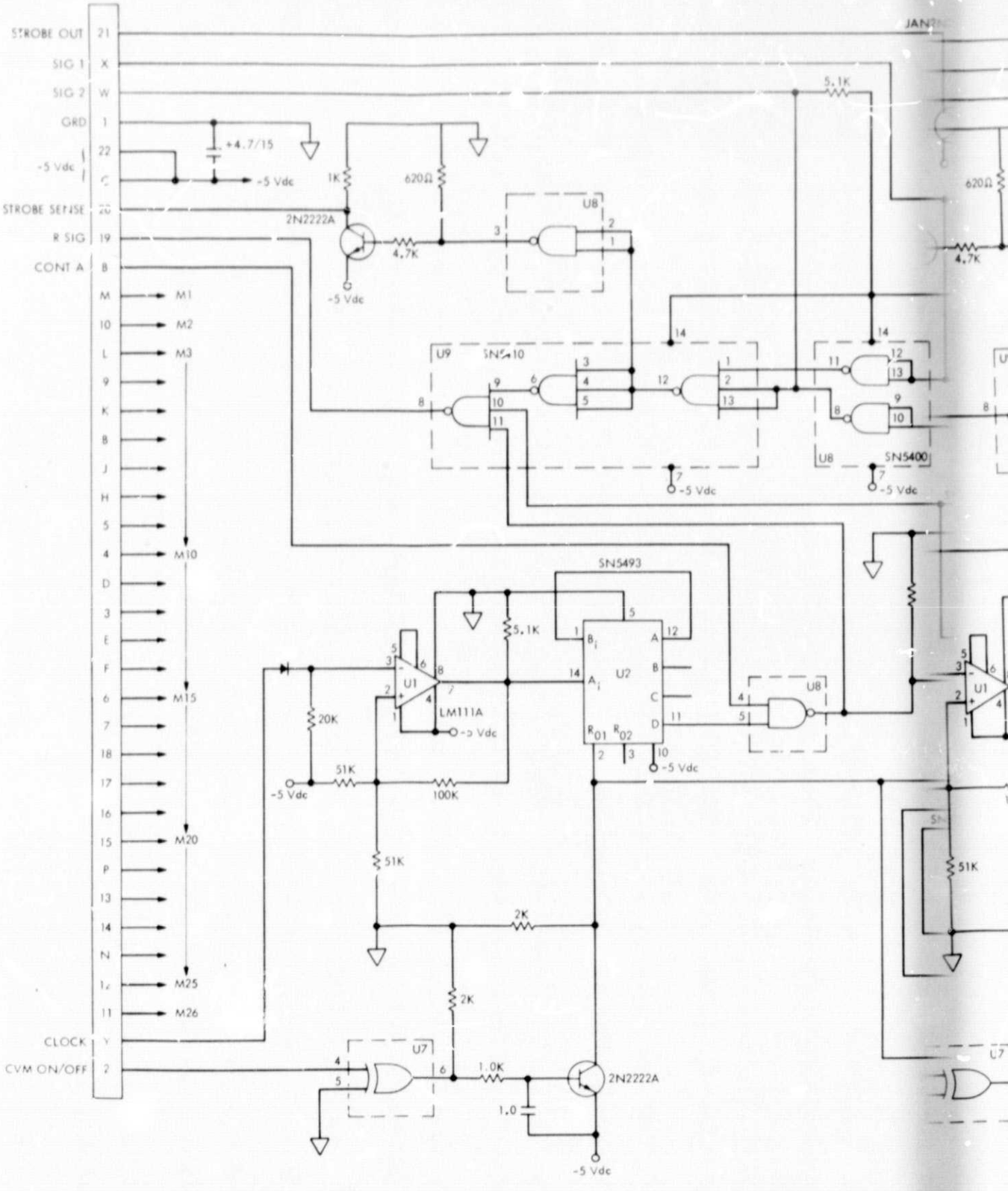

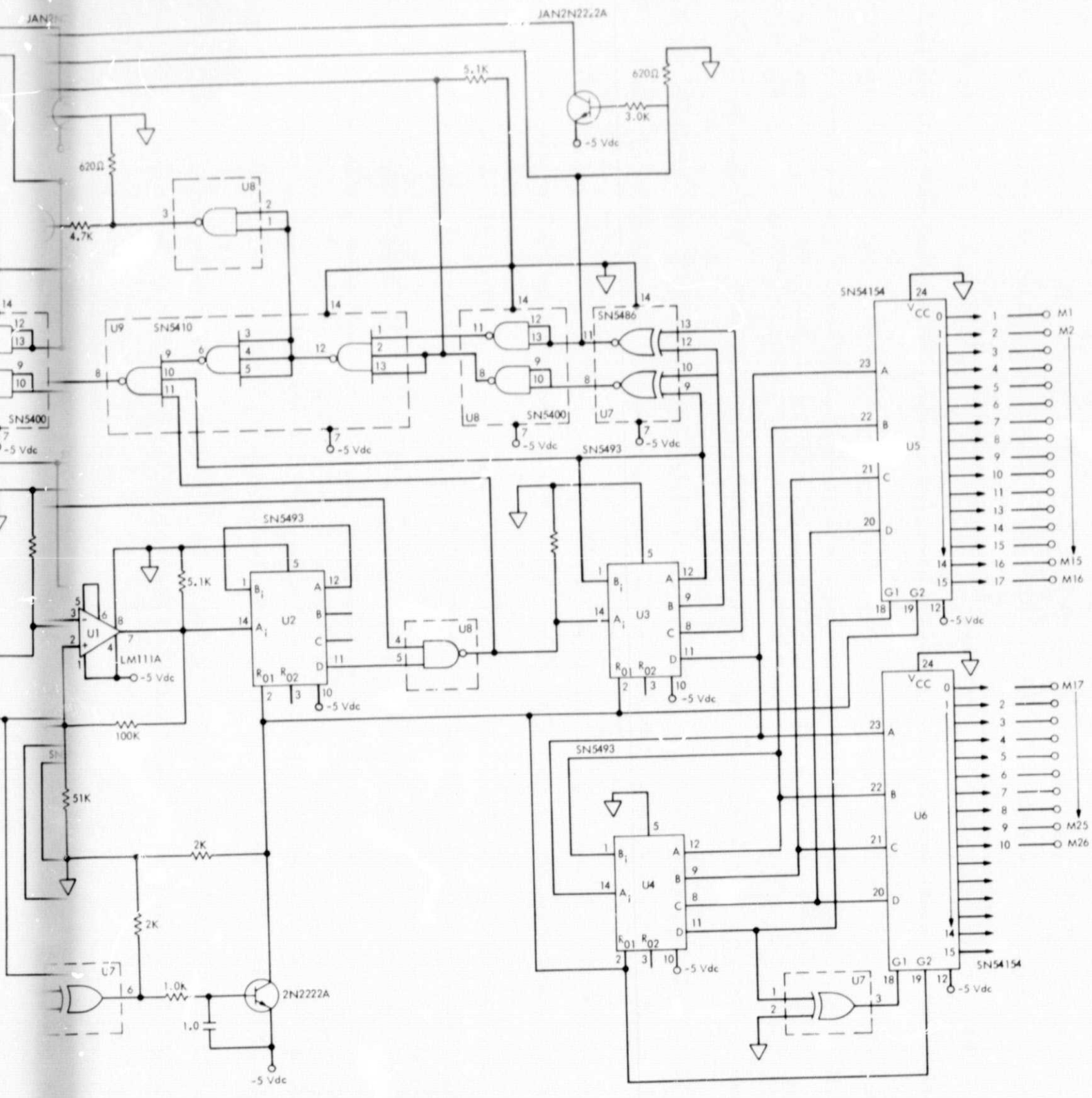

ORIGINAL PAGE IS
OF POOR QUALITY

Figure 5-3. Multiplexer Schematic (MUX, B2)

PRECEDING PAGE BLANK NOT FILMED.

FOLDOUT FRAME 1

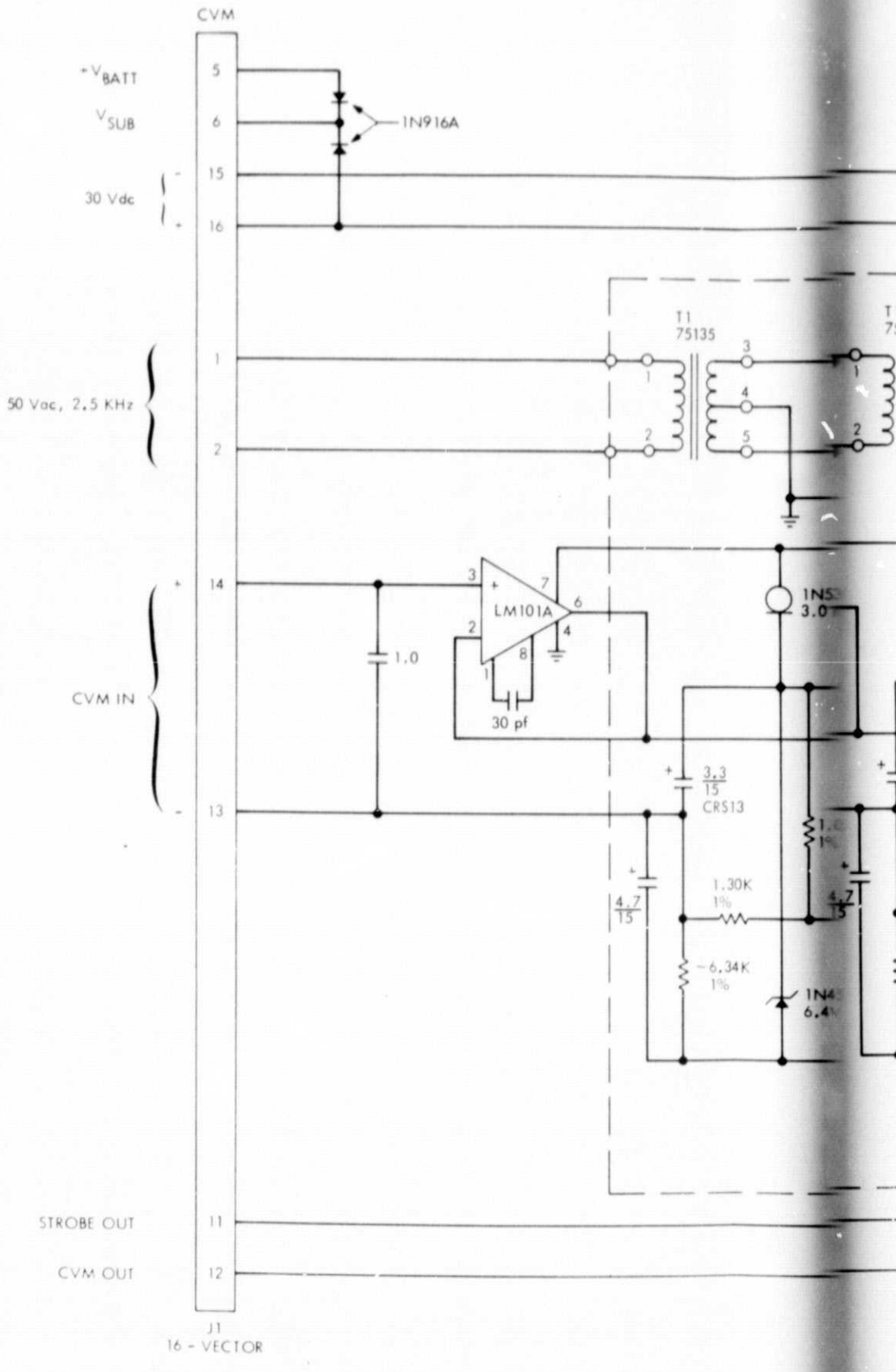

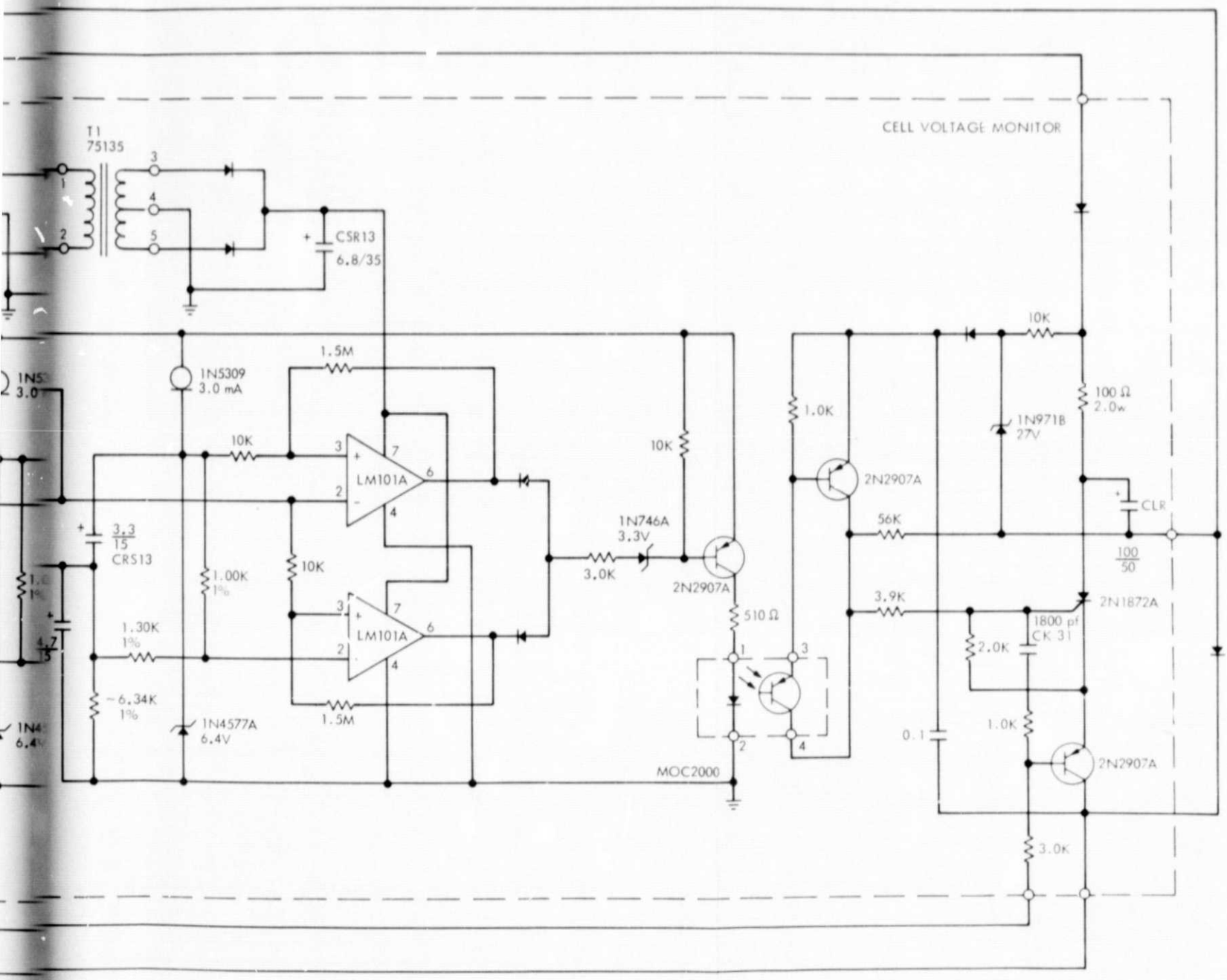

Figure 5-4. Cell Voltage Monitor (CVM, B1)

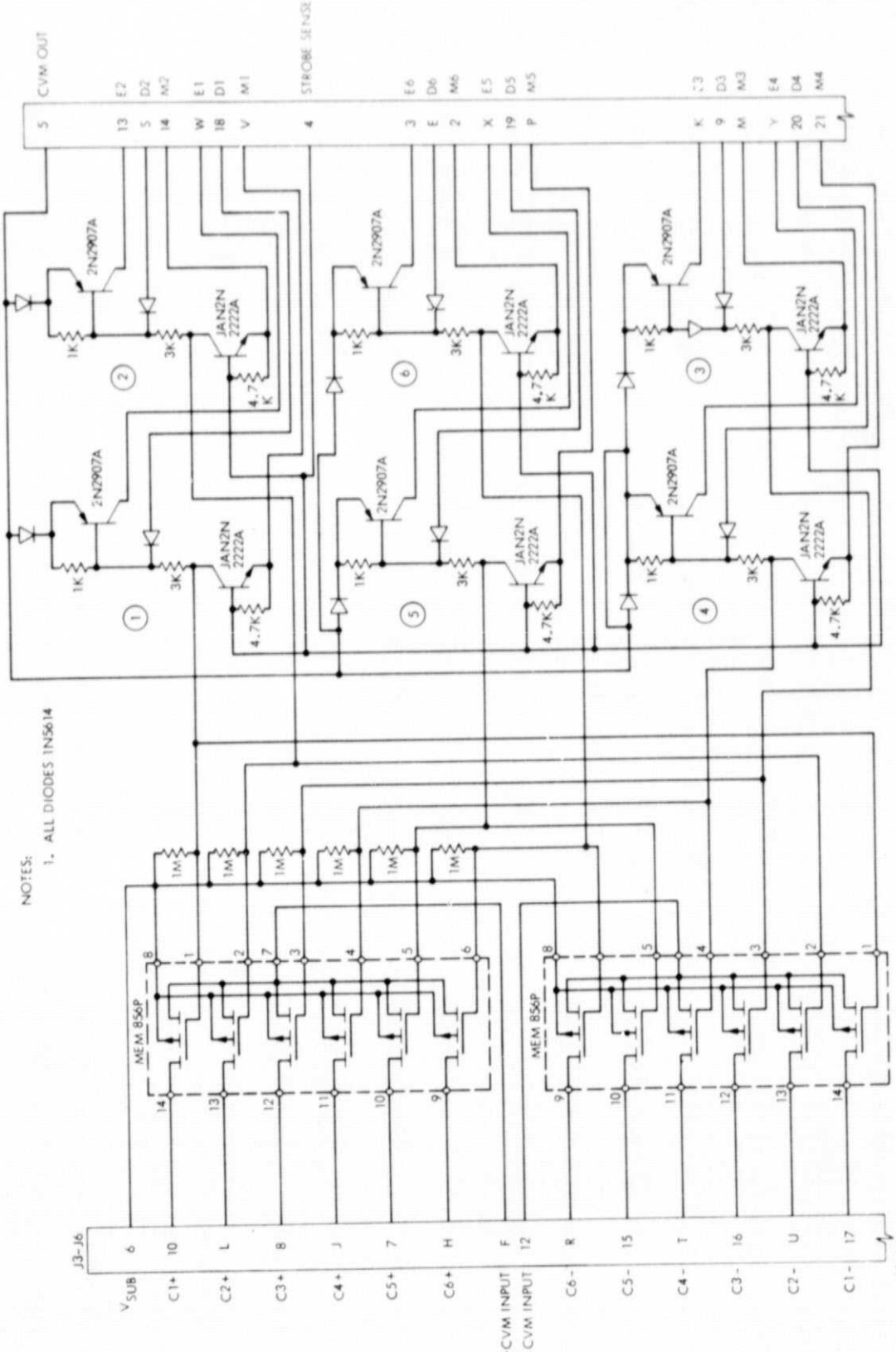

Figure 5-5. 6-Channel FET Switch and Driver Board Schematic

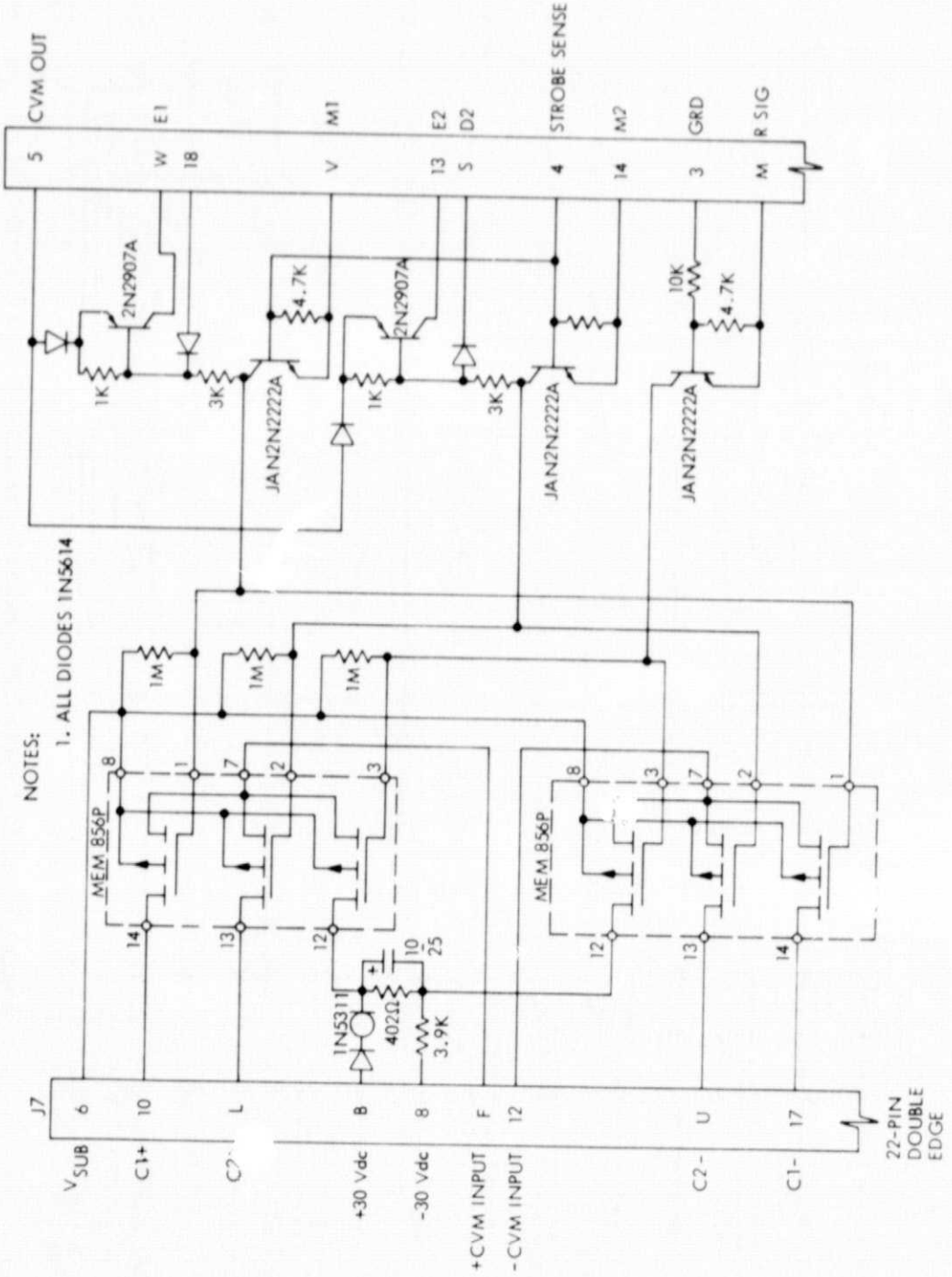

Figure 5-6. TWO Channel FET Switch and Driver Board Schematic (B7)

FOLDOUT FRAME 1

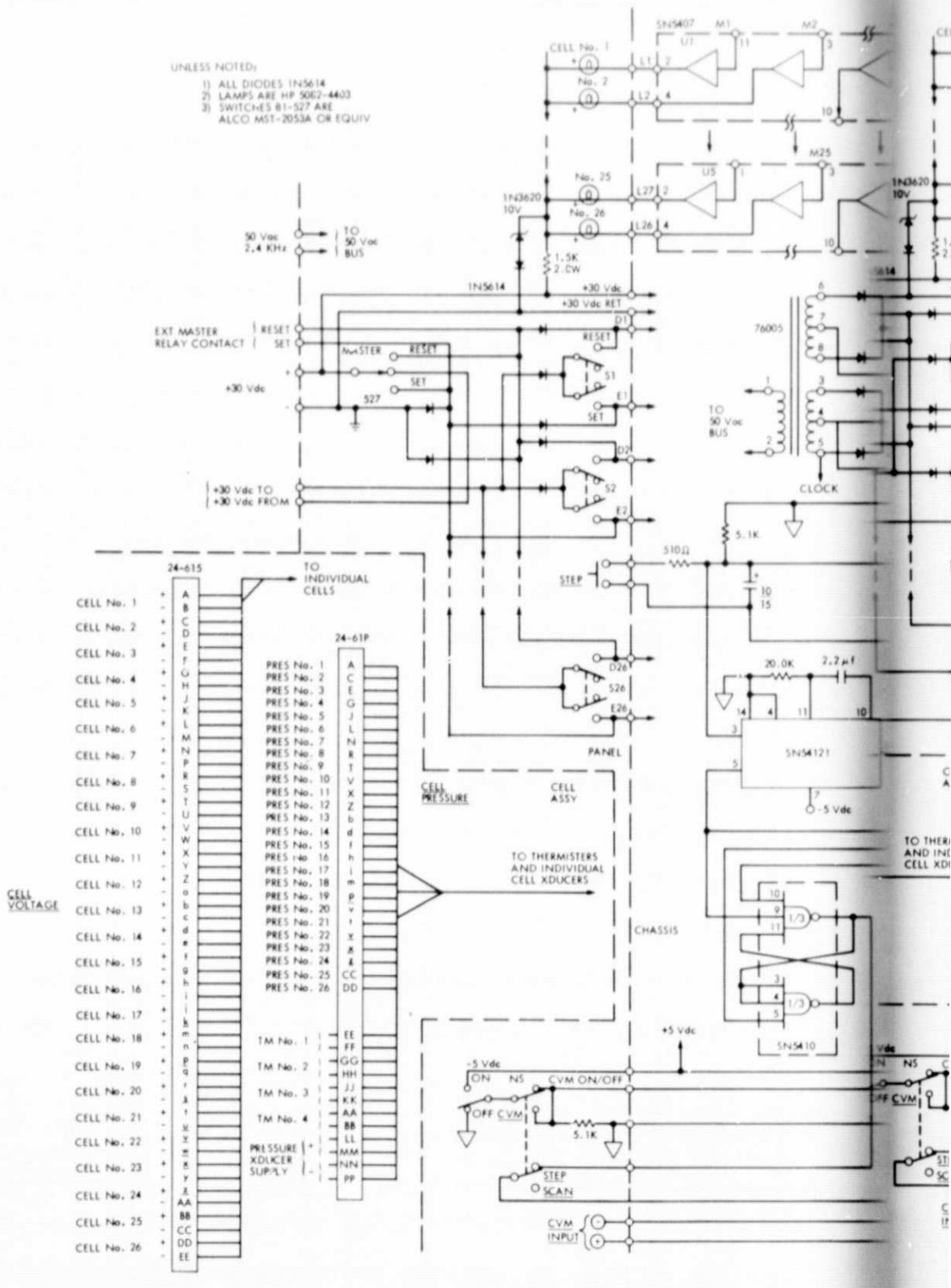

PRECEDING PAGE BLANK NOT FILMED

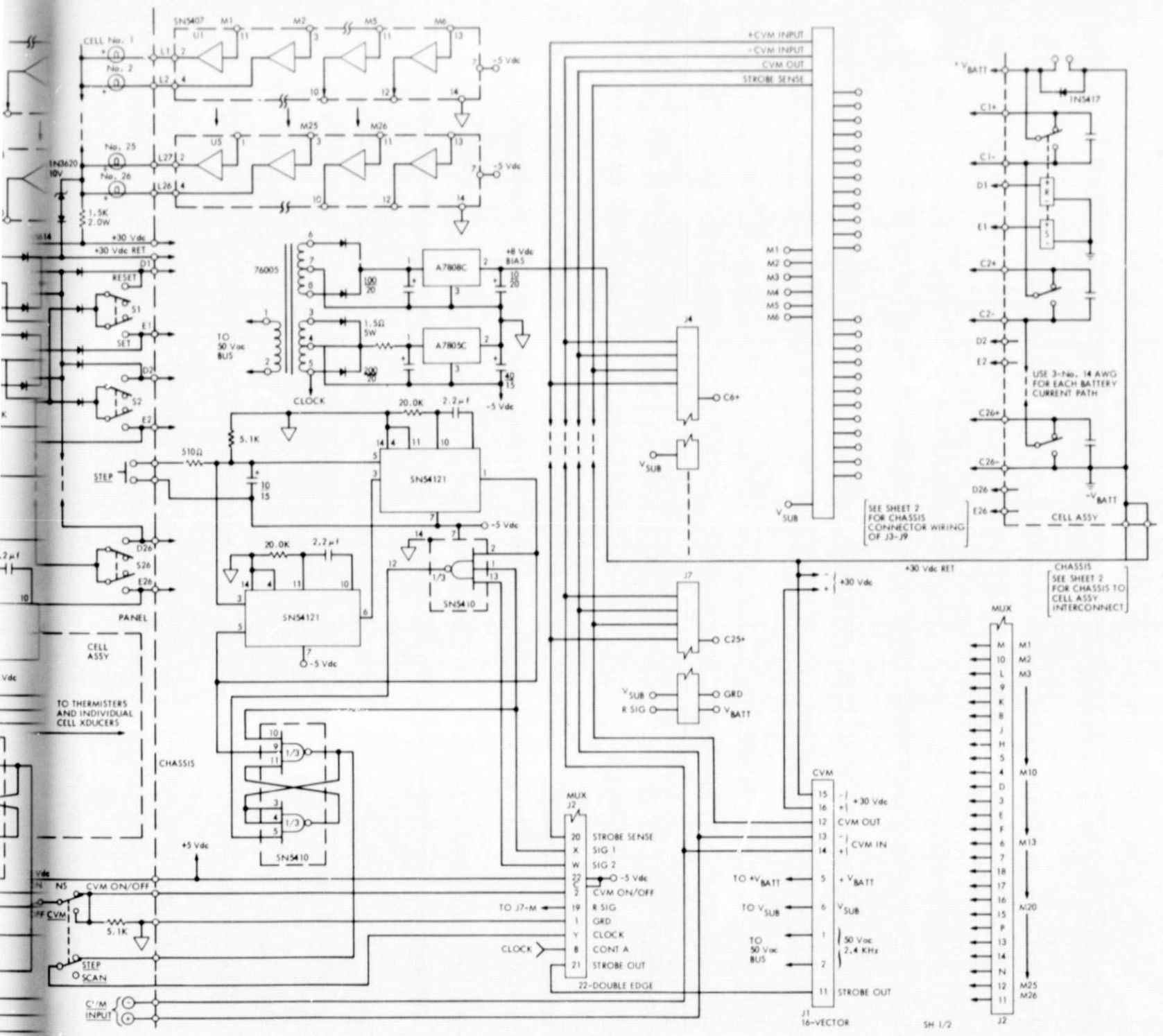

Figure 5-7. Detailed Schematic of 26-Cell Control System

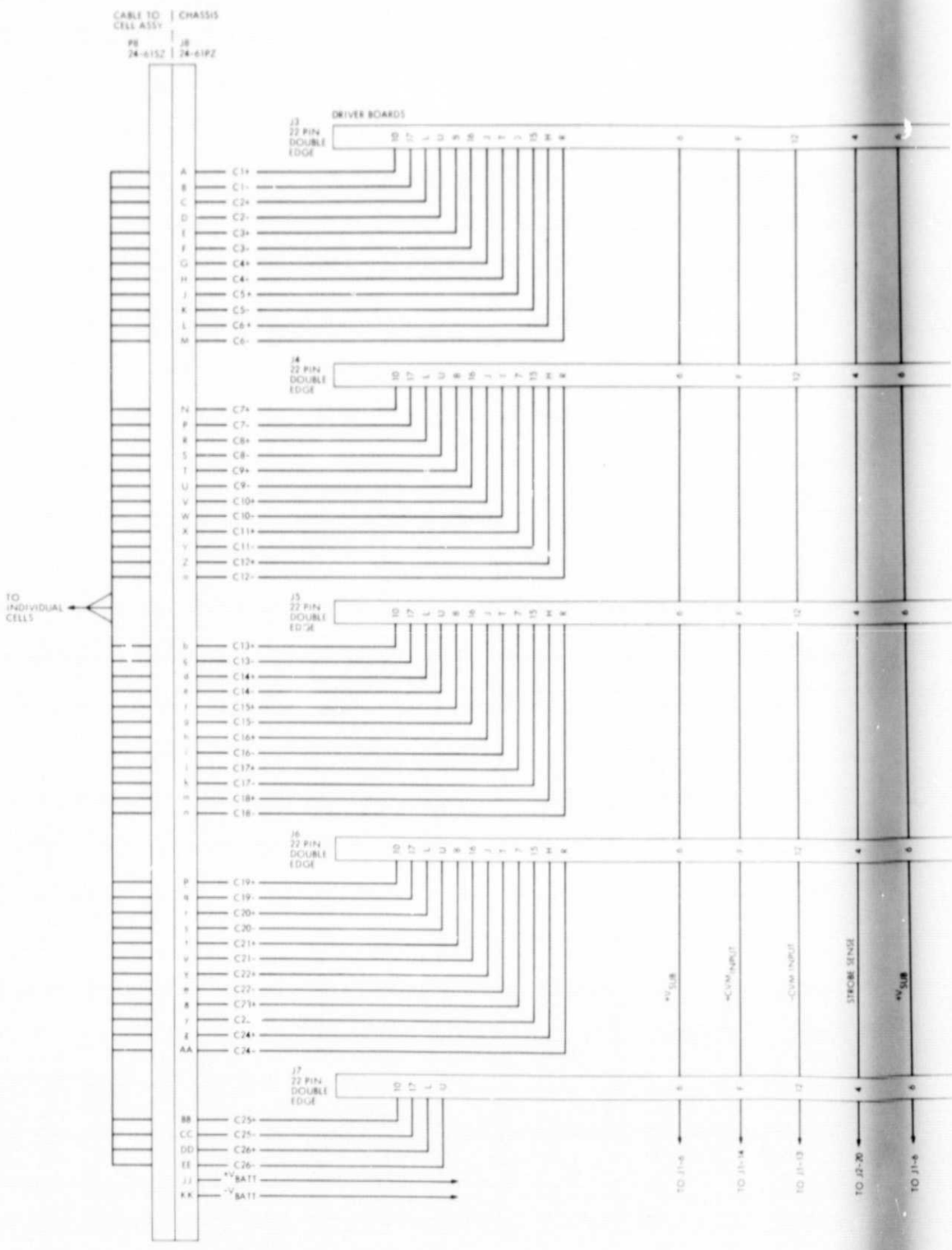
CABLE TO CELL ASSY
CHASSIS
P8 24-6152
J8 24-6192
DRIVER BOARDS
J3 22 PIN DOUBLE EDGE
J4 22 PIN DOUBLE EDGE
J5 22 PIN DOUBLE EDGE
J6 22 PIN DOUBLE EDGE
J7 22 PIN DOUBLE EDGE
TO INDIVIDUAL CELLS
A C1+
B C1-
C C2+
D C2-
E C3+
F C3-
G C4+
H C4-
J C5+
K C5-
L C6+
M C6-
N C7+
P C7-
R C8+
S C8-
T C9+
U C9-
V C10+
W C10-
X C11+
Y C11-
Z C12+
a C12-
b C13+
c C13-
d C14+
e C14-
f C15+
g C15-
h C16+
j C16-
k C17+
l C17-
m C18+
n C18-
P C19+
q C19-
r C20+
s C20-
t C21+
u C21-
v C22+
w C22-
x C23+
y C2_
z C24+
AA C24-
BB C25+
CC C25-
DD C26+
EE C26-
JJ +V BATT
KK -V BATT
+V SUB
+COM INPUT
-COM INPUT
STROBE SENSE
+V SUB
TO J1-6
TO J1-14
TO J1-13
TO J2-20
TO J1-6

[illegible] FRAME 2

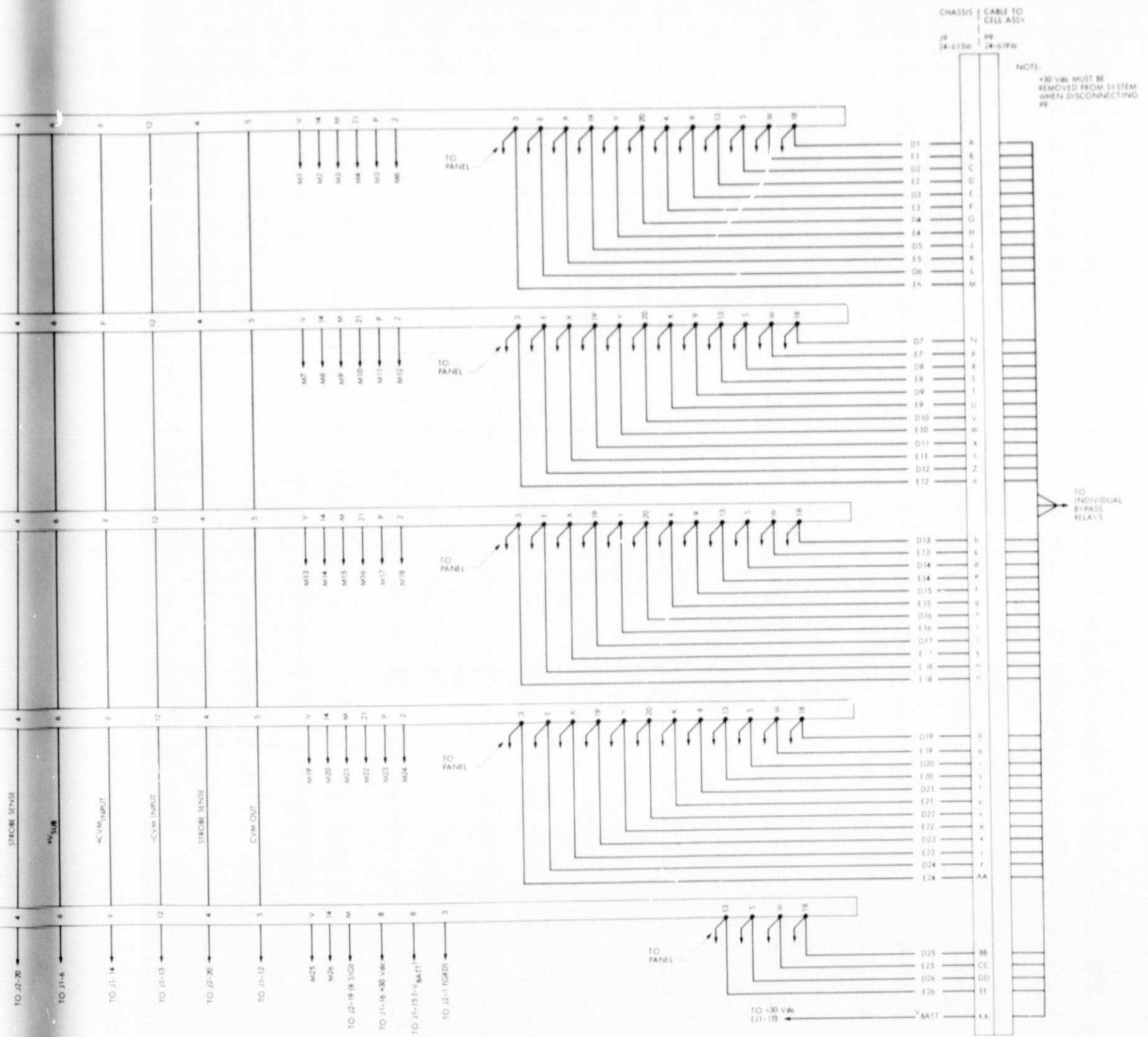

Figure 5-8. Connector Wiring for 26-Cell Control System

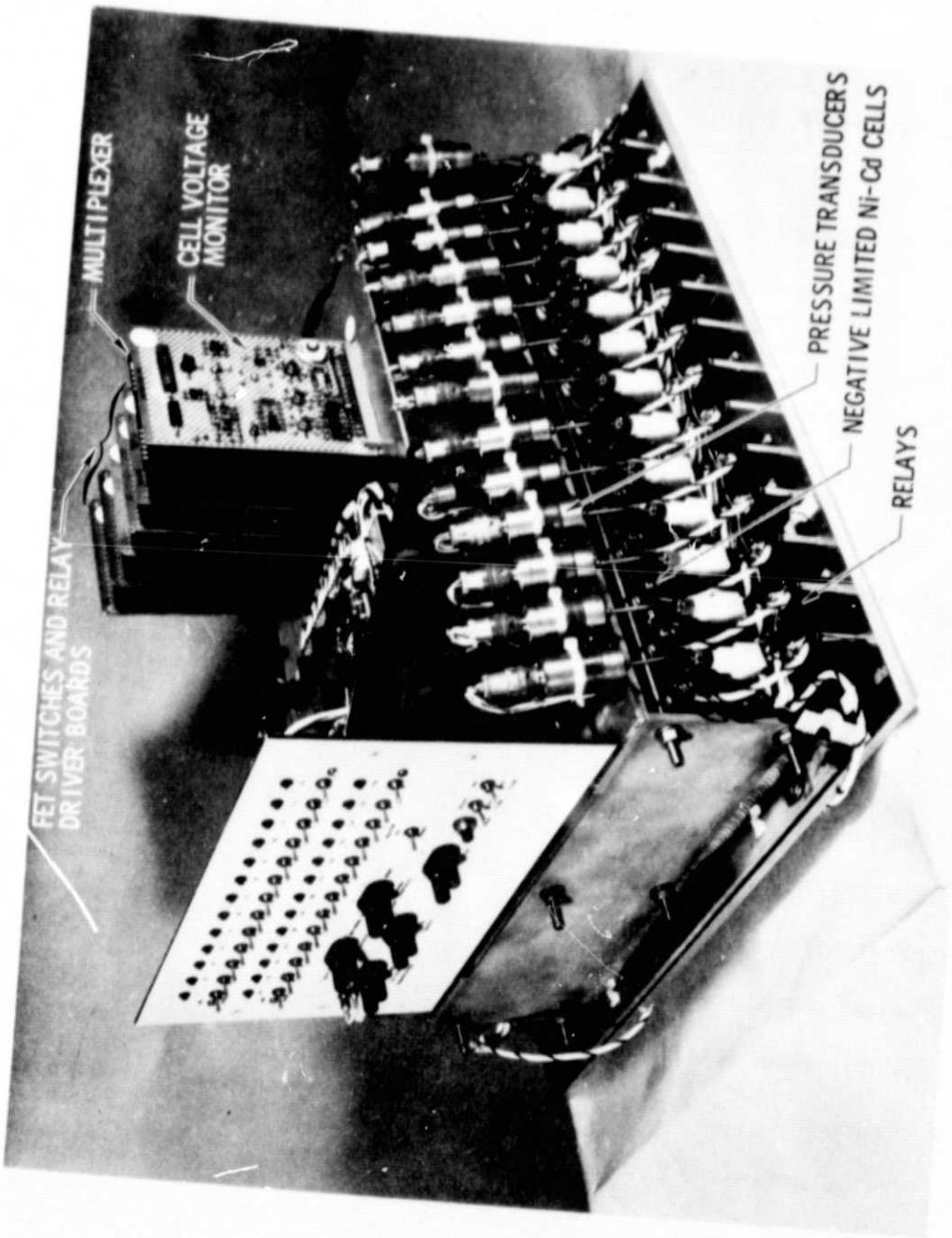

Figure 5-9. 26-Cell Breadboard Battery with Bypass Electronics

schematic of the overall 26-cell control system. Figure 5-8 is a connector wiring diagram for the 26-cell control system. Finally, Figure 5-9 is a photograph of the completed breadboard system comprised of 26 Negative Limited Ni-Cd cells and bypass electronics. Parts count of the electronics was 12 parts per cell, and weight was about 68 g/cell, including relays.

The Cell Voltage Monitor (CVM) (B1) is a window comparator that is sequentially connected to each cell by means of an array of P-channel, enhancement-type Metal Oxide Semiconductor Field Effect Transistors (MOSFET) which are controlled by the Multiplexer (MUX) and its associated logic. The CVM is floating with respect to all voltages in the system and will float to the voltage level of the particular cell being monitored. This eliminates the troublesome, large common-mode rejection problem encountered when using a fixed referenced voltage monitor. This CVM isolation is provided by a transformer-coupled power supply and an optically coupled output drive signal. An SCR switch is used to reduce drive power requirements for the relays and provide more positive switching. A 100 μfd storage capacitor is provided to activate the relay of a failed-open cell, should the +30 VDC supply be derived from the battery terminals. At present, however, the +30 VDC is derived from an external source.

The MUX is a 26-channel logic circuit, deriving its clock input from a countdown of the 2.4 KHz input power. The occurrences within each 53.33 msec frame allotted to the monitoring of each cell are shown in the logic diagram of Fig. 5-2. For illustration, the beginning of each Cell 2 frame is used as a starting point. At this point, the CVM is disconnected. After 6.67 msec, the strobe sense signal connects

Cell 2 to the CVM input. After an allotted 6.67 msec for the CVM to float and settle at the proper level, and also for the cell voltage to charge the CVM input filter capacitor of 1.0 μf through the MOSFET "ON" resistance, the strobe out signal connects the output of the CVM to the set coil on Cell 2. This condition will be maintained for 26.67 msec, allowing time for the relay to pull in, should the monitored cell be out of tolerance. After this, the strobe out signal disconnects the CVM output, and 6.67 msec later the strobe sense signal disconnects Cell 2 from the input. After 6.67 msec, Frame 2 terminates and Frame 3 is initiated; the previous cycle of occurrences then begins again. All 26 cells are scanned every 1.676 sec.

On this breadboard system, provisions are made to monitor any one selected cell without a continuous scanning of the cells. This is initiated by switching to the STEP mode. This locks the CVM to Cell 1, with both input and output of the CVM connected. Pressing the STEP pushbutton, a 30 msec one-shot is initiated, releasing the locked condition (Figure 5-2). Signal CONT A is generated from the one-shot output, Sig. 1, and Sig. 2. This allows the MUX to progress to Cell 2 and lock up there when CONT A goes low. Pressing the STEP pushbutton again allows the process to repeat and move on to Cell 3, and so on. Since only 26 channels of a 32-channel multiplexer circuit are used, Cell 1 will not repeat after Cell 26, but the STEP pushbutton must be pressed an additional 6 times to rearrive at Cell 1.

The control logic block contains a double one-shot configuration to eliminate any anomalies caused by contact bounce of the STEP push-button switch. An R-S flip-flop is used to prevent any noise pickup in the wiring between MUX, the control logic board, and panel, which allows the MUX to run freely.

The FET switch and relay driver boards (B3-B7) (Figure 5-5) contain 26 identical circuits (B3-B6 contain 6 circuits each, while B7 contains 2 circuits and a "dummy" cell). This dummy cell is nominally 1.4 VDC and is provided to reset the CVM comparators at the end of each frame by the R signal. At present, power to this dummy cell is provided from the +30 VDC supply, but would probably be best derived from the 2.4 KHz so it could float along with the CVM. Each circuit accepts its appropriate M signal and the strobe sense signal from the MUX. It provides the dual function of switching the appropriate 2-FET switches connecting the desired cell terminals to the CVM input, and also steering the CVM output to the corresponding bypass relay set coil.

The enhancement-type MOSFETs used are the General Instrument Corp. type MEM856. These are 80-volt devices fully capable of handling the expected maximum battery voltage of 45 volts, plus an additional +13 VDC gate bias. They are enhancement-type FETs which are normally OFF and, therefore, no battery current drain or cell shorting can result with a power glitch in the gate circuit for whatever reason. Also, they are packaged 6 FETs in a DIP or flat-pack, providing reduced parts count and size.

The relay used is the Leach JCL SPDT type, with 25-amp contacts. Weight of each is 40 g each, or 1.04 kg for 26 relays.

In operation, the CVM ON/OFF switch in the OFF position disengages the MUX circuitry, and no cell or relays are connected to the CVM. The STEP/SCAN switch may be in any desired position when switching the CVM ON/OFF switch to ON, with Cell 1 being the first cell connected. With 50 VAC and +30 VDC power being applied with the CVM ON/OFF switch in the ON position, Cell 1 will probably not be the first cell encountered. It is recommended that this switch be in the OFF position when applying power.

The STEP pushbutton allows monitoring of each cell individually, as desired, with the STEP/SCAN switch in the STEP position. The illuminated lamp indicates the cell being monitored. In the SCAN position, the sequential flashing of the lamps indicates the system multiplexing action.

Relay control, other than the CVM set coil excitation, is provided from three additional sources:

(1) Individual relay set and reset control is provided by a center-OFF toggle switch assigned to each cell, located on the panel below each lamp. Moving this switch to the reset position overrides any signal from the CVM attempting to set the relay.

(2) The master relay control switch, also a center-OFF toggle switch, provides the capability of set and reset for all relays simultaneously. This overrides the CVM output, individual relay control, and the external master relay control.

(3) The external master relay control provides remote set and reset capabilities when used with equipment such as a data acquisition system. (When this feature is not in use, a shorting bar must be inserted in the EXT RELAY CONTACT banana jack pair.)

B. TEST AND EVALUATION

The 26-cell breadboard battery was first subjected to short-term charge-discharge cycles to check functionality of the bypass control system. The cycles included intentional periods of overcharge and deep discharge to insure that all cells switched from the operating to the bypass mode at both the high and low prescribed voltages. After a few minor adjustments, it was established that the system was working well as all cells were found to be switched to the bypass condition at 1.75 $\pm$ .05 volts on charge and at 0.90 $\pm$ .05 volts on discharge.

At this point, the battery was readied for two additional tests. The first of these was designed to observe its performance over a long-term, simulated planetary mission. The second was designed to observe its performance in a simulated earth orbiting mission.

1. Simulated MM-71 Mission

The battery was installed in an environmental chamber maintained at 13°C (55.4°F) and carried through the sequence of events encountered by the actual 26-cell M-71 battery. Overall battery voltage, current, and temperature as well as individual cell voltages and internal pressures were recorded on a Non-Linear Systems data acquisition system. The sequence of events consisted of: a) a prelaunch cycle, b) a launch

discharge and recharge, c) a first midcourse correction discharge and recharge, d) a cruise period, e) a second midcourse correction discharge and recharge, and f) an orbit insertion discharge and recharge. The test was carried out over a 10-month period from June 1976 to March 1977. Since the Negative Limited Ni-Cd battery cells were known to be degraded, the discharge currents employed in the various maneuvers were less (about one half) than those employed in the actual M-71 battery.

The simulated prelaunch cycle consisted of discharge at 2.0 amp for 1.0 hr, followed by recharge at 2.0 amp until all cells attained the bypass condition. Terminal battery voltages at the start and at the end of the 2-hr discharge period were 33.6 and 31.4 volts, respectively, with no indications that any of the cells had achieved the bypass condition. Terminal battery voltage during the recharge portion of the cycle is given in Figure 5-10. Shape of the voltage was typical for all subsequent recharge periods and was as anticipated in the design stages. During the first two-thirds of the charge period (0 to 40 min) the voltage was noted to rise gradually from about 33 to 39 volts, with no indications that any of the cells achieved the bypass condition. During the final third of the charge period (40 to 64 minutes), the voltage began to rise at a somewhat more rapid rate (to 45 volts in 56 minutes), and then, as the individual cells were bypassed, the apparent terminal voltage dropped sharply to 0 volt at the end (64 minutes). During the final 8 minutes, all cells achieved the bypass condition and were effectively removed from the circuit.

The simulated launch discharge was carried out two days after the simulated prelaunch cycle. Current and time for the maneuver were 6.0 amp and 60 minutes, respectively. Battery terminal voltage (Figure 5-11)

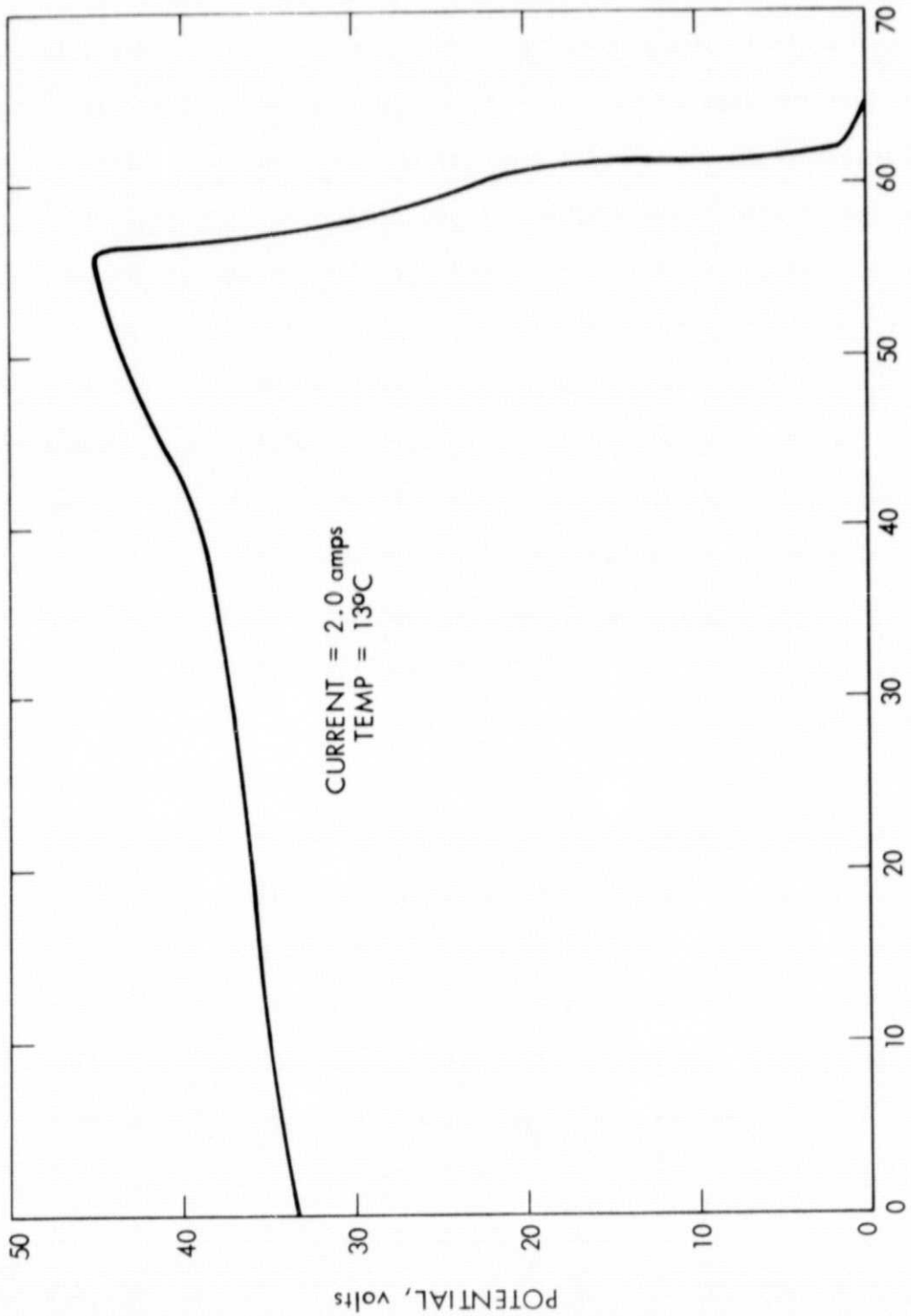

Figure 5-10. Recharge of Breadboard Battery during Prelaunch Cycle

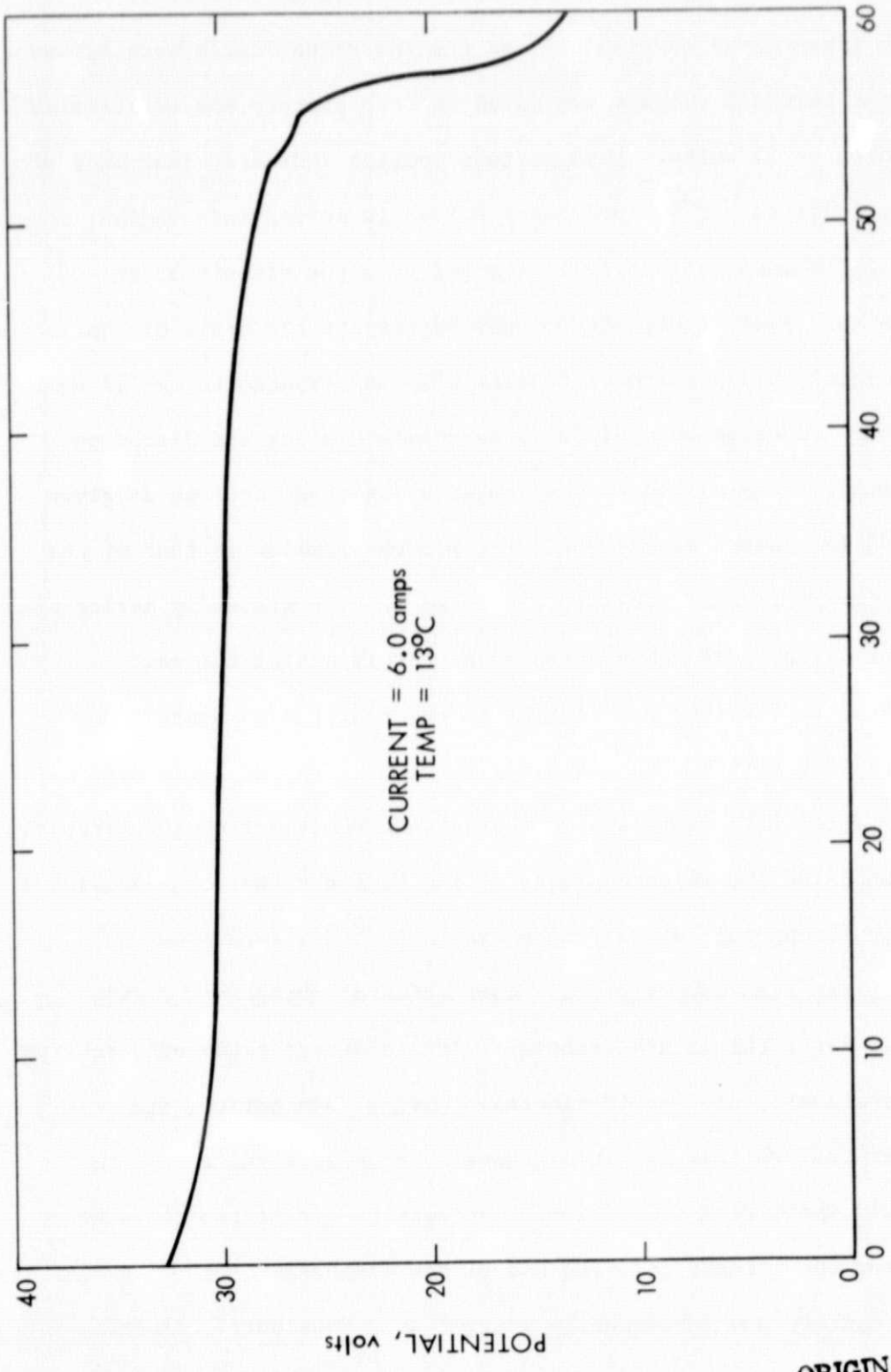

Figure 5-11. Launch Discharge of Breadboard Battery

was noted to drop gradually, like the actual MM-71 battery during the first 53 minutes of discharge (from about 33 volts to 28 volts). Thereafter (from 53 to 60 minutes), as the individual cells were bypassed, the apparent terminal voltage was noted to drop sharply and erratically from 28 volts to 13 volts. This voltage decline indicated that many of the cell potentials had dropped below 0.9 volts during this period, and these cells were automatically removed from the circuit by the bypass control system. Capacity of the battery at the 6-amp discharge rate to a cutoff of 26 volts (1.0 volt/cell) is computed to be 5.7 A-hr.

Battery recharge was initiated immediately after the discharge launch period. Terminal battery voltage during this recharge is given in Figure 5-12. Shape of the voltage trace was similar to that of the prelaunch charge period. Voltage was noted to rise gradually during the first 140 minutes to 38 volts, then more sharply during the next 12 minutes to 41.5 volts, and finally to apparently drop sharply and erratically to 0 volt during the final 25 minutes as the individual cell voltages reached 1.75 volts and the cells were removed from the circuit. From the shape of the voltage trace, it can be shown that the individual cell charge acceptance values ranged from 5.1 to 5.9 A-hr.

The first simulated midcourse correction discharge was carried out one day after the launch recharge. This maneuver required discharge of the battery at 6 amp for 50 minutes. During this period, the battery terminal voltage declined gradually from 33.1 volts to 23.3 volts. There were indications that perhaps one or two cells were removed from the circuit near the end of the discharge.

The battery was subsequently charged at 2 amps until all cells were in the bypass condition, then discharged again at 6.0 amp until

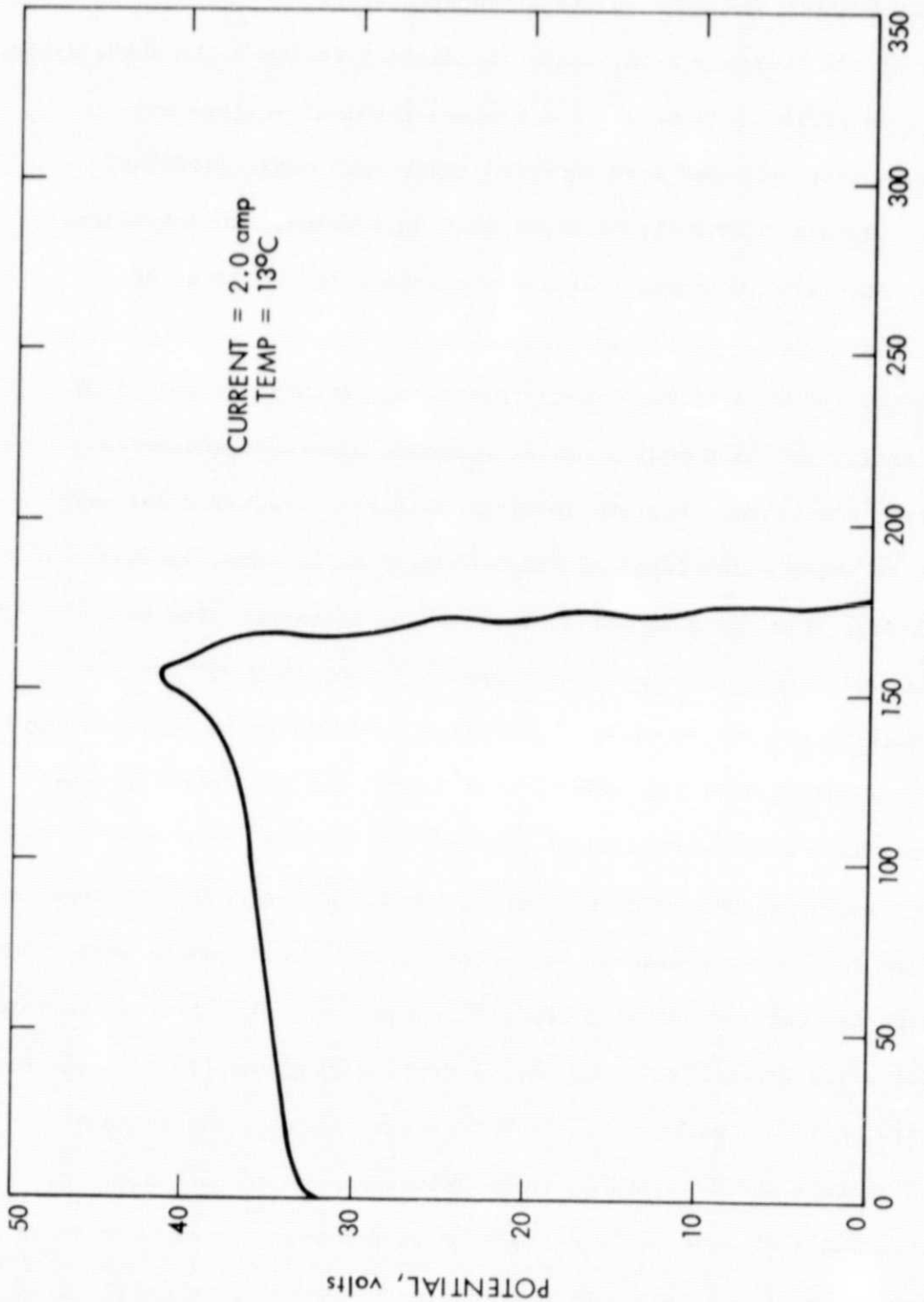

Figure 5-12. Recharge of Breadboard Battery after Launch Discharge

all cells were in the bypass condition. Terminal voltage characteristics during this cycle were similar to those encountered in the launch cycle.

The battery was left in the discharged state for the initial portion of the cruise period, which immediately followed the above cycle. During this period (189 days), the battery terminal voltage and individual cell voltages were recorded twice each week. Terminal voltage remained relatively constant near 32.6 volts, and individual cell voltages also remained relatively constant in the range of 1.24 to 1.26 volts for this 189-day period.

After 190 days of simulated cruise, the battery was placed on charge at 2.0 amp in preparation for a second simulated midcourse correction discharge. Battery terminal voltage characteristics were similar to those encountered in prior charges at 2.0 amp, i.e., a gradual rise from 32 to 38 volts, followed by a sharper rise to 42 volts and, finally, a very sharp apparent drop to 0 volt as the individual cells were bypassed. The first cell was noted to reach the bypass condition after 176 minutes (5.8 A-hr), and the last cell was noted to reach the bypass condition after 326 minutes (10.9 A-hr). These results signified that both the bypass system and the cells appeared to remain in good working order. The second simulated midcourse correction discharge was carried out at 6 amp for 1 hour. Battery terminal voltage declined quite gradually from 34 to 27 volts during the first 52 of the 60-minute period. During the last 8 minutes, however, the voltage dropped sharply and erratically to 15 volts. These results indicated that potentials of some cells dropped below 0.9 volts after 52 minutes (5.2 A-hr), and the bypass system effectively removed these cells from the circuit after this time.

At the completion of the second simulated midcourse correction discharge, the battery was left in the discharged state for the second portion of the simulated cruise period, whichlasted for an additional 35 days. The battery terminal voltage and individual cell voltages were recorded twice each day. Terminal voltage again remained relatively constant (near 32.8 volts), and individual cell voltages also remained relatively constant in the range of 1.24 to 1.27 volts during this 35-day period.

On the 226th day of the mission, the battery was placed on charge at 2.0 amp in preparation for the simulated orbit insertion maneuver. Battery terminal voltage characteristics were very similar to those encountered in the charge period preceding the midcourse maneuver. The simulated orbit insertion discharge was carried out at 4.5 amp until all cells had attained the bypass condition. Figure 5-13 gives terminal voltage characteristics for this discharge. Voltage was noted to drop gradually from 34 to 30 volts during the first 60 minutes and sharply and erratically thereafter to 120 minutes. These results signify that the bypass system was once again effective in removing cells with low voltage from the circuit.

The actual MM-71 mission included additional maneuvers requiring battery discharge, including: a) orbit trims, b) occultation discharges during orbiting, and c) antenna-pointing maneuvers. Simulation of these additional maneuvers was deemed unnecessary, since functionality of the bypass system had already been demonstrated over the long term. Further, it was at this point desired to test the system under rapid cycling conditions, such as in earth orbit.

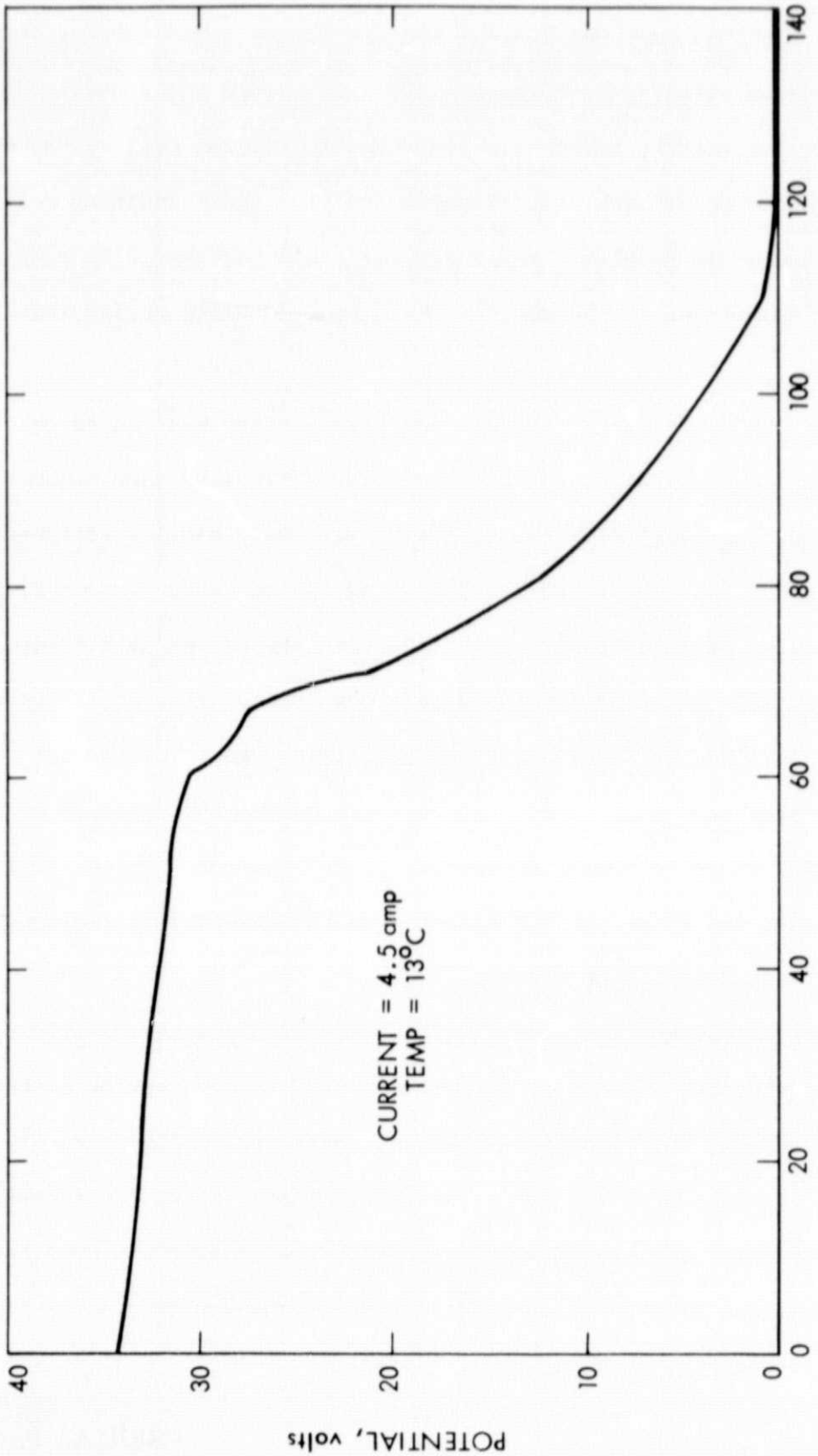

Figure 5-13. Orbit Insertion Discharge of Breadboard Battery

A final point is that throughout the 226 days of the simulated mission, the internal pressures of all cells remained near 1.0 kg/cm^2, and reached a maximum of only 1.5 kg/cm^2 at the end of the charge periods.

2. Low Earth Orbit Cycling

At this point, the battery was placed on a continuous rapid-cycle regime to simulate operation in low earth orbit. The regime consisted of charge at 3.2 amp for 60 minutes, followed by discharge at 6.0 amp for 30 minutes. The environmental chamber in which the battery was installed had become inoperative, so the test was carried out at room temperature near 21°C. Overall battery, current, and temperature as well as individual cell voltages and internal pressures were recorded on a Non-Linear Systems data acquisition system.

Figure 5-14 gives the voltage profile of one of the battery cells on Cycle No. 1000, after which the test was terminated. During discharge, cell voltage was maintained above 0.90 volts, so that the cell remained in the circuit. During the later states of charge, the cell voltage exceeded the 1.75 volt limit, so that the bypass system automatically removed the cell from the circuit. Cell voltage was noted to drop sharply to the open circuit potential and remain at this level until the start of the subsequent discharge period.

Figure 5-15 gives the voltage profile of another of the battery cells on Cycle No. 1000. During the mid-point of discharge, cell voltage was noted to drop below the 0.90 volt limit, so that the bypass system automatically removed the cell from the circuit. Cell voltage was noted to rise sharply to the open circuit potential and remain at this level until the start of the subsequent charge period. During this

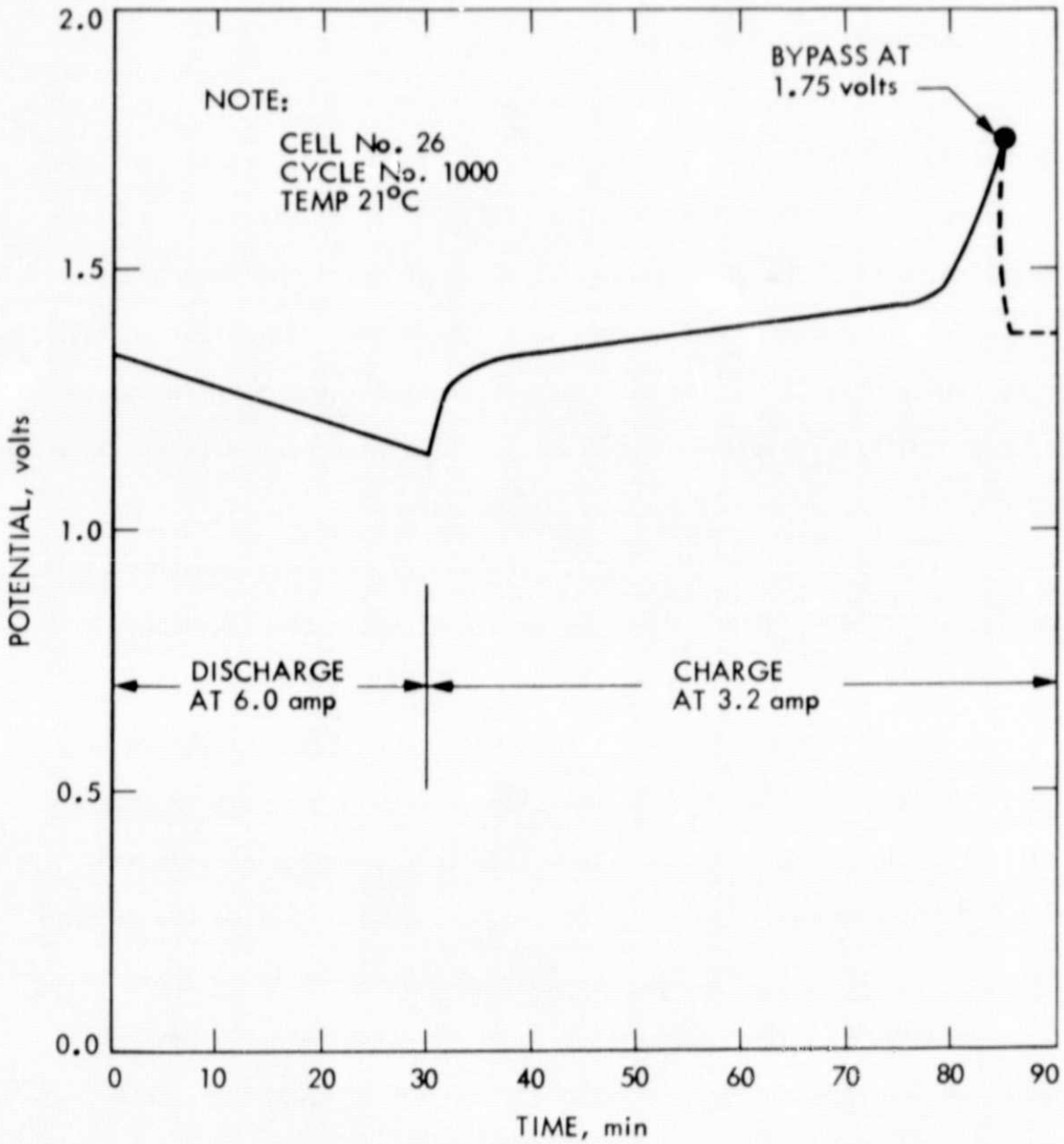

Figure 5-14. Example of Bypass on Charge during Low Earth Orbit Cycling

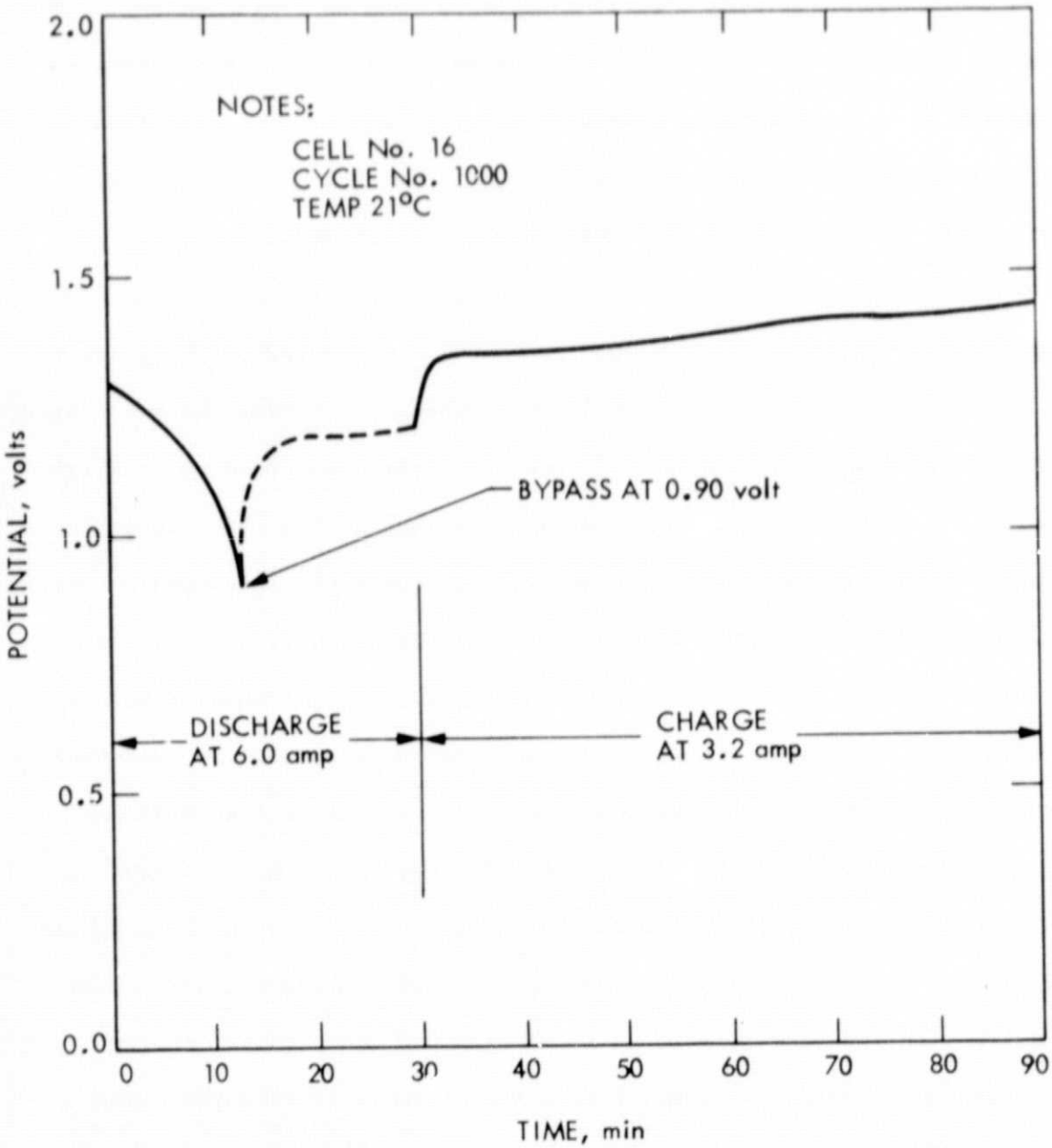

Figure 5-15. Example of Bypass on Discharge during Low Earth Orbit Cycling

period, the cell voltage did not exceed 1.75 volts, so that the cell remained on charge for the complete 60 minutes.

Figure 5-16 gives the voltage profile of the complete battery during the early states of the test on Cycle No. 33 and on final Cycle No. 1000. During discharge on the 33rd cycle, the voltages of all cells remained above 0.90 volts for the complete 30 minutes, and none were removed from the circuit. During charge on the 33rd cycle, the voltages of all cells remained below 1.75 volts for the first 58 minutes, and none were removed from the circuit. Apparent battery terminal voltage was noted to drop sharply to 0.00 volt during the final 2 minutes of charge on the 33rd cycle as the individual cells were bypassed. During the early stages of discharge on Cycle 1000, the terminal voltage was noted to be slightly more than 1 volt less than the terminal voltage during the 33rd cycle. Explanation for this phenomenon was that one cell had developed an internal short and was permanently removed from the circuit. During the final stages of discharge on the 1000th cycle, the voltages of several cells fell below 0.90 volts, and these were automatically removed from the circuit. Battery terminal voltage was noted to drop accordingly below 20 volts by the end of this period. During the early stages of charge on Cycle No. 1000, the terminal voltage was noted to be slightly more than 1 volt less than the terminal voltage during the 33rd cycle. Explanation for this phenomenon is the same as above, i.e., one cell was shorted and permanently removed from the circuit. During the final stages of the 1000th charge cycle, the voltages of several cells exceeded 1.75 volts, and these were automatically removed from the circuit. Apparent battery terminal voltage was noted to drop accordingly below 20 volts by the end of this period.

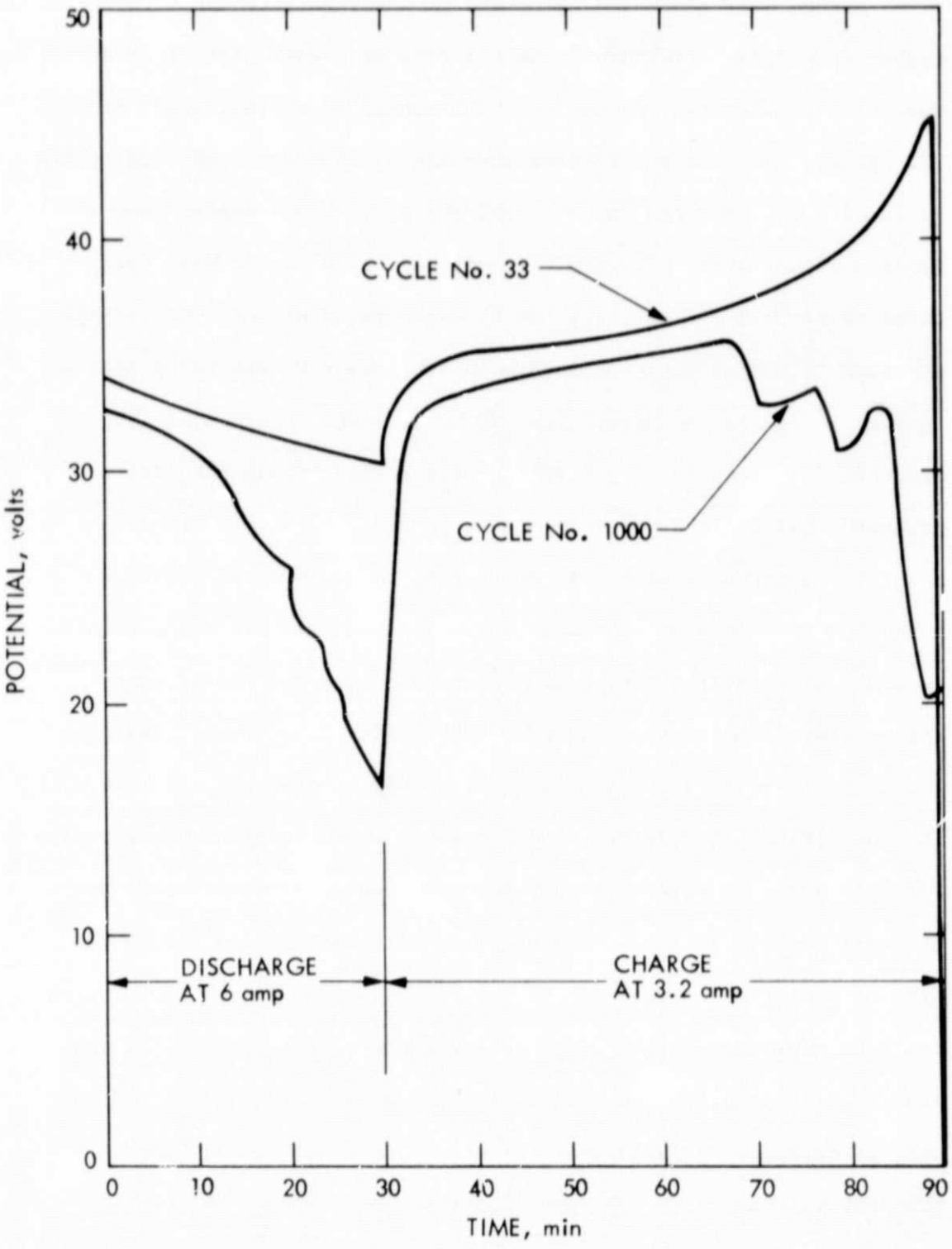

Figure 5-16. Terminal Voltage of Breadboard Battery during Low Earth Orbit Cycling

Figure 5-17 gives the variation of internal pressure with the number of cycles. Pressure in Cell 8 (the cell with highest pressure) was noted to increase sharply with the number of cycles, until about 200 cycles, and then to increase more slowly when the number of cycles exceeded 200. From the shape of the curve, it would appear that a maximum steady state pressure of about 2.9 kg/cm^2 would have been obtained in Cell 8 if cycling had been continued beyond 1000 cycles. Pressure in Cell 23 (the cell with lowest pressure) was noted to rise sharply to 1.5 kg/cm^2 after about 200 cycles and then gradually decay thereafter. Pressure in all other cells varied within the limits of pressures for Cells 8 and 23.

The internal pressure is controlled by the rate of hydrogen evolution and hydrogen recombination. The hydrogen evolution occurs in small amounts from the cadmium electrode near the end of each charge period when cell voltage is approaching 1.75 volts. Hydrogen recombination occurs continuously and slowly by chemical reaction with the positive active material. The rate of recombination must increase with pressure, as this would explain the attainment of a steady state pressure in Cell 8, i.e., when the rate of recombination equals the rate of evolution. The decay in pressure of Cell 23 after 200 cycles could be explained on the basis of development of a partial internal short. At this point the cell does not become fully charged and its voltage remains low throughout the charge period; the cell does, thereafter, not evolve hydrogen at the end of charge. The decay in pressure is then attributed to chemical reaction of the hydrogen that was evolved during the first 200 cycles.

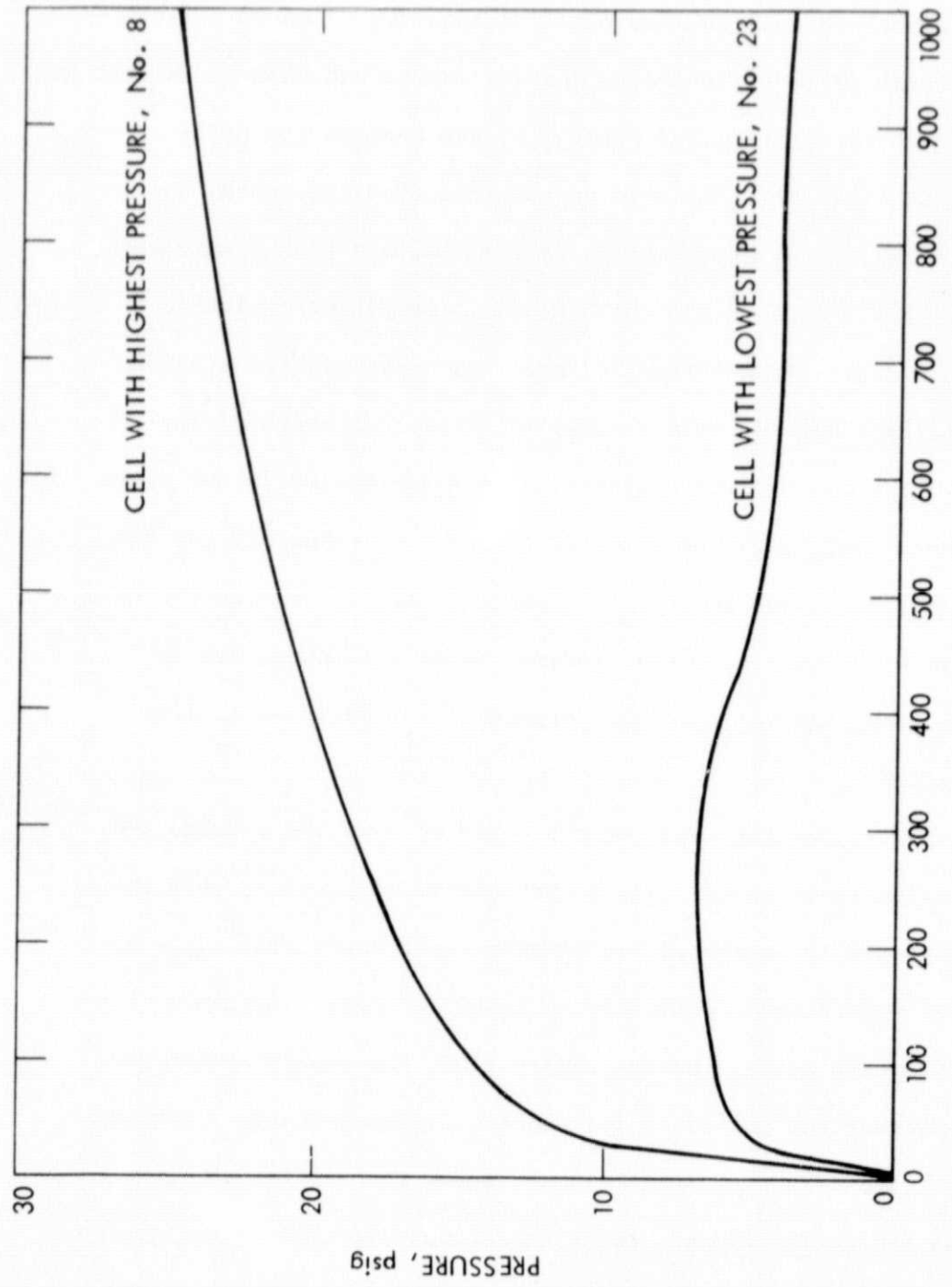

Figure 5-17. Variation of Internal Pressures with Number of Low Earth Orbit Cycles

3. Additional Remarks on Tests

From an overall power systems point of view, the above test results are both encouraging and discouraging, depending on the criteria.

In terms of specific energy density (wh/Kg and wh/cm^3) as well as coulombic density (A-hr/Kg and A-hr/cm^3), the results are quite unimpressive. This is attributed to the fact that the energy and coulombic densities of the complete system, battery plus electronics, are appreciably less than the corresponding energy and coulombic densities of state-of-the-art Ni-Cd systems. Further, the specific output densities degrade more rapidly with use than state-of-the-art batteries. The low specific outputs are not attributed in any large degree to size and weight of the electronics, but rather to the low output of the Negative Limited Ni-Cd battery cells. To make the system competitive with existing Ni-Cd systems, it will be necessary to considerably upgrade the specific outputs of the Negative Limited battery cells.

From a reliability and control point of view the results are, however, quite impressive. This is attributed to the fact that the system successfully completed two lengthy tests under what might be considered "worst case" conditions, i.e., with extreme imbalance among the battery cells. During this period, the bypass system was used extensively and performed its function without mishap. Maximum pressure attained in any given cell was noted to be only 2.9 kg/cm^2. If the system had malfunctioned, there would undoubtedly been much more extensive internal gassing and pressure rise; and in all likelihood, catastrophic cell failures.

In summary, it has been shown that the bypass system is of sound design and functions well, while the Negative Limited battery cells

are severely lacking in performance capability. The combination of the two does not yet look promising from a power systems point of view. The bypass system could, however, be advantageously employed at the present time to improve reliability of other types of existing batteries.

SECTION VI

PROPOSED FLIGHT SYSTEM

A block diagram of a proposed flight system is given in Figure 6-1. Functionally, the system is very similar to the 26-cell breadboard, without the various control functions. All external control is shown in one logic block. Using available diode and transistor packaged arrays and resistor network packages, a flight systems electronic parts count is estimated at 150 parts, or about 6 parts per cell. Total weight of electronics is estimated at 1.63 kg or about 64 g/cell. Further reduction in parts count and weight could be achieved with development of costlier customized hybrid circuits.

At present, the CVM is designed to detect a fixed discernible voltage level, such as would be the case for the Negative Limited Ni-Cd cells or silver cells, etc. Should a tighter tolerance temperature, pressure, and/or cycling-compensated, voltage-sensing level be required as for a conventional Ni-Cd cell, the CVM would have to be redesigned with these features incorporated. The CVM would be required to have greater noise immunity, resulting in more input filtering and a slower scan rate of the cell array. Also, a Farady-shielded transformer for the CVM power supply would be in order. Careful consideration of wiring and shielding of cell sense leads must be taken. Also, the substrate voltage for the MOSFET switch must be controlled very carefully to avoid any signal modulation from this potential source.

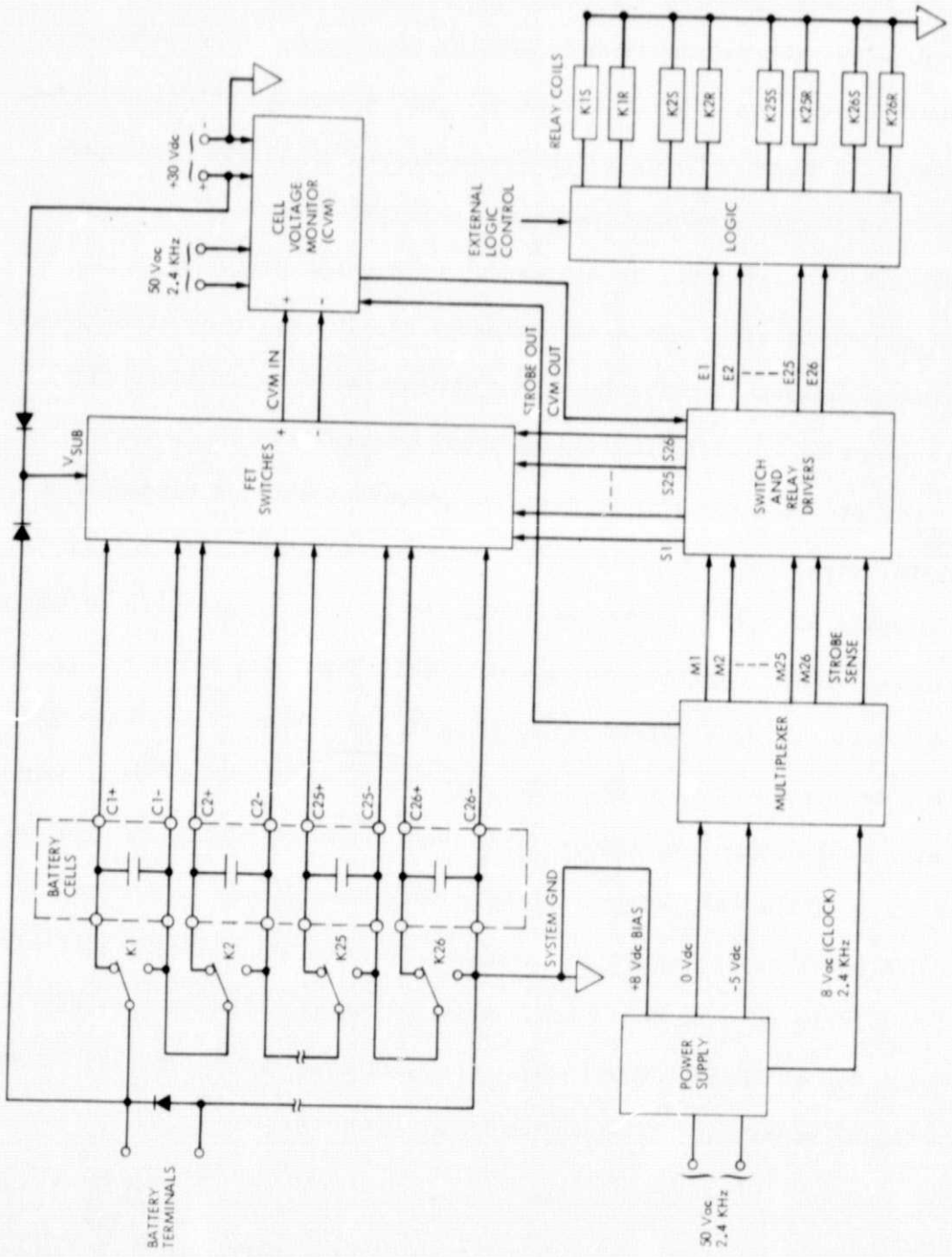

Figure 6-1. Functional Block Diagram - Proposed Flight 26-Cell Battery Charge Control System

SECTION VII

CONCLUSIONS

A breadboard-type bypass control system was developed to control a battery comprised of 26 Negative Limited Ni-Cd cells. Major elements of the system consisted of a cell voltage monitor, a multiplexing circuit, and individual electromechanical relays for each of the 26 battery cells. The system was designed to automatically remove from the circuit any cell with voltage in excess of $1.75 \pm .05$ volts on charge, and with voltage below $0.90 \pm .05$ volts on discharge. The bypass system was found to function well in controlling the cells during the course of a simulated 10-month MM-71 mission and also during 2 months of simulated low earth orbit cycling. Maximum pressure attained in any given cell was only 2.9 kg/cm^2 during this period. A flight version of the bypass system is estimated to have a total parts count of 150 and a total weight of 1.63 kg. When fully developed, the system shows promise for improving life and reliability of spacecraft batteries.

The Negative Limited Ni-Cd cells were found to deliver much lower than their rated capacity as received, and their capacities were found to degrade quite rapidly with use. Deliverable energy densities at completion of the simulated mission tests were only a fraction of corresponding energy densities of state-of-the-art Ni-Cd cells. Considerable upgrading in performance of the Negative Limited Ni-Cd cells will be necessary before they can be considered for flight applications.

SECTION VIII

RECOMMENDATIONS

1) In its present state of development, the bypass system appears essentially ready for incorporation in flight systems employing sealed Ag-Zn and Ag-Cd cells.

2) With some modifications of the cell voltage monitor to give it greater noise immunity (see Sec VI), it would be ready for incorporation in systems employing conventional sealed Ni-Cd cells.

3) When performance of the Negative Limited Ni-Cd cells is upgraded to that of conventional sealed Ni-Cd cells, the battery bypass control system could then be recommended for incorporation in flight systems employing this type of cell.

4) The technology developed on this project is directly applicable to another JPL effort designated as the Automated Power Systems Management Program. It is recommended that this technology be transferred to that program.

SECTION IX

REFERENCES

1. "Fabrications and Testing of Negative-Limited Sealed Nickel-Cadmium Cells," Final Report on JPL Contract No. 953680, Gould, Inc., Mendota Heights, Minn., 31 March 1975.

2. Bogner, R. S., "Mariner Mars 1971 Battery Design, Test, and Flight Performance," JPL Technical Memorandum 33-591, 15 April 1973.

NASA-JPL-Coml, L.A., Calif